PB81-191124

Areal Prediction of Water and Solute Flux in the Unsaturated Zone

Arizona Univ., Tucson

Prepared for

Robert S. Kerr Environmental Research Lab.
Ada, OK

Apr 81

U.S. Department of Commerce
National Technical Information Service
NTIS.

TECHNICAL REPORT DATA
(Please read Instructions on the reverse before completing)

1. REPORT NO.	2.	3. RECIPIENT'S ACCESSION NO
EPA-600/2-81-058	ORD Report	PB81-191124

4. TITLE AND SUBTITLE	5. REPORT DATE
Areal prediction of water and solute flux in the unsaturated zone.	April 1981
	6. PERFORMING ORGANIZATION CODE

7. AUTHOR(S)	8. PERFORMING ORGANIZATION REPORT NO.
Arthur W. Warrick Azizolah Amoozegar-Fard	

9. PERFORMING ORGANIZATION NAME AND ADDRESS	10. PROGRAM ELEMENT NO.
Department of Soils, Water and Engineering The University of Arizona Tucson, AZ 85721	1BB770
	11. CONTRACT/GRANT NO.
	Grant No. R-804751

12. SPONSORING AGENCY NAME AND ADDRESS	13. TYPE OF REPORT AND PERIOD COVERED
Robert S. Kerr Environmental Research Laboratory Office of Research and Development U.S. Environmental Protection Agency Ada, Oklahoma 74820	Final
	14. SPONSORING AGENCY CODE
	EPA/600/15

15. SUPPLEMENTARY NOTES

16. ABSTRACT

The areal distributions of water and solutes over land was studied. This was done by examining data sets available from previous studies as well as by flow simulations. Most of the simulations of salt and water movement were by the "crude" Monte Carlo technique. For infiltration, "Philip's" formula was solved once in a scaled form, after which results were algebraic without repeating the laborious steps. Similarly, drainage calculations were made very efficient by utilizing a scaled form of the nonlinear moisture flow equation. Salt distributions were considered for cases of equal irrigation amounts, but with intake rates varying over space. Deterministic calculations based on the mean velocity and apparent diffusion coefficient gave erroneous results for both fluxes and distributions of salts in the profile. The true average distribution is much more dispersed with more salts reaching deep depths and also more salts near the surface. Similarly, the mass emissions of salts averaged over a field appears earlier than would be calculated by using mean velocities.

17. KEY WORDS AND DOCUMENT ANALYSIS

a. DESCRIPTORS	b. IDENTIFIERS/OPEN ENDED TERMS	c. COSATI Field/Group
Water Water Resources Soil Irrigation Statistics Simulation Drainage	spatial variability solute flux soil-water flux Monte Carol techniques geostatistics	48/E 68/D 72/F

18. DISTRIBUTION STATEMENT	19. SECURITY CLASS *(This Report)*	21. NO. OF PAGES
RELEASE TO PUBLIC	Unclassified	88
	20. SECURITY CLASS *(This page)*	22. PRICE
	Unclassified	

EPA Form 2220-1 (9-73)

BEGIN FIRST LINE OF TEXT HERE
TYPING GUIDE SHEET
CENTER OF PAGE
TOP OF IMAGE AREA
DROPPED HEAD; BEGIN SECTIONS HERE
6-1/2"
9-1/8"
BEGIN LAST LINE OF TEXT
3/8"
BOTTOM OF IMAGE AREA; OUTSIDE DIMENSION FOR TABLES AND ILLUSTRATIONS

PB81-191124

EPA 600/2-81-058
April 1981

AREAL PREDICTION OF WATER AND SOLUTE FLUX IN THE UNSATURATED ZONE

by

Arthur W. Warrick
and Azizolah Amoozegar-Fard
Department of Soils, Water and Engineering
The University of Arizona
Tucson, Arizona 85721

Grant No. R-804751

Project Officer

Arthur G. Hornsby
Source Management Branch
Robert S. Kerr Environmental Research Laboratory
Ada, Oklahoma 74820

ROBERT S. KERR ENVIRONMENTAL RESEARCH LABORATORY
OFFICE OF RESEARCH AND DEVELOPMENT
U.S. ENVIRONMENTAL PROTECTION AGENCY
ADA, OKLAHOMA 74820

REPRODUCED BY
NATIONAL TECHNICAL INFORMATION SERVICE
U.S. DEPARTMENT OF COMMERCE
SPRINGFIELD, VA. 22161

EPA-287 (Cin.)
(4-76)

BEGIN FIRST LINE OF TEXT HERE
TYPING GUIDE SHEET
CENTER OF PAGE
TOP OF IMAGE AREA
DROPPED HEAD BEGIN SECTIONS HERE
6-1/2"
3-1/8"
BEGIN LAST LINE OF TEXT
BOTTOM OF IMAGE AREA OUTSIDE DIMENSION FOR TABLES AND ILLUSTRATIONS
3/8"
PAGE NUMBER
EPA-297 (Cin.)
(4-76)

DISCLAIMER

This report has been reviewed by the Robert S. Kerr Environmental Research Laboratory, U.S. Environmental Protection Agency, and approved for publication. Approval does not signify that the contents necessarily reflect the views and policies of the U.S. Environmental Protection Agency, nor does mention of trade names or commerical products constitute endorsement or recommendation for use.

BEGIN FIRST LINE OF TEXT HERE
TYPING GUIDE SHEET
CENTER OF PAGE
TOP OF IMAGE AREA
DROPPED HEAD; BEGIN SECTIONS HERE

FOREWORD

Environmental protection efforts dealing with agricultural and nonpoint sources have received increased emphasis with the passage of the Clean Water Act of 1977 and the subsequent implementation of the Rural Clean Water Program. As part of this Laboratory's research on the occurrence, movement, transformation, fate, impact and control of environmental contaminants, data and analytical methodologies are developed to assess the causes of and possible solutions to environmental effects of irrigated agriculture.

This report addresses the spatial variability of water and solute fluxes and its relationship to environmental sampling in the unsaturated (vadose) zone. Some environmental parameters vary to a large degree in space and time, requiring special consideration in sampling and intrepretation. This project is a step toward developing more cost-effective techniques, such as "geostatistics," which can be applied to these problems. This research should stimulate further developments in the academic community and solve pollution problems related to pollutant transport in soil systems.

Clinton W. Hall
Director
Robert S. Kerr Environmental Research Laboratory

BEGIN LAST LINE OF TEXT
BOTTOM OF IMAGE AREA; OUTSIDE DIMENSION FOR TABLES AND ILLUSTRATIONS
3/8"

EPA-287 (Cin.)
(4-76)

BEGIN FIRST LINE OF TEXT HERE
TYPING GUIDE SHEET
CENTER OF PAGE
TOP OF IMAGE AREA
DROPPED HEAD: BEGIN SECTIONS HERE

ABSTRACT

The purpose of this project was to evaluate distributions of water and salt fluxes over areas of land. The primary interest was with regard to irrigated lands as affected by salinization, crop environment and water and salts returning to ground or surface sources. The project relied on data available in the literature and no field research was conducted. In the main, the study was in three parts: (1) observations of distributions for a variety of soil physical parameters and inference on sampling; (2) simulations of water and salt flux for non-deterministic systems; and (3) a sensitivity analysis for drainage. Most of the effort was in Part 2.

Simulations of water and salt fluxes were made using the "crude" Monte Carlo technique. For infiltration, "Philip's" formula was utilized in a scaled form, was solved one time and simulations run algebraically without repeating the laborious steps. Similarly, results for the nonlinear drainage case were solved based on only one finite difference determination. The Monte Carlo simulation was carried out by simple interpolation from the one nonlinear solution. Unfortunately, no great short-cut was found for cyclic or seasonal irrigation regimes, although some interesting results based on linearized solutions were found for high frequency applications.

Salt distributions were calculated for cases of equal irrigation amounts over time but with intake rate varying over space. Deterministic calculations based on the mean velocity and apparent diffusion coefficient give erroneous results compared to the "average" values over the field for either salt profiles or fluxes. The true "average" by depth for a given time is much more dispersed with more salts reaching very deep depths and also with more salts remaining close to the surface. Similarly, the mass emission of salts averaged over a field for a given depth appear earlier in time and taper off more gradually for a pulse input than deterministic calculations based on mean velocities would indicate.

This report was submitted in fulfillment of Grant No. R-804751 by the University of Arizona, Tucson, under the sponsorship of the U.S. Environmental Protection Agency. This report covers a period from September 1, 1976, to February 28, 1979, and work was completed as of January 30, 1980.

BOTTOM OF IMAGE AREA; OUTSIDE DIMENSION FOR TABLES AND ILLUSTRATIONS
BEGIN LAST LINE OF TEXT
3/8"

EPA-287 (Cin.)
(4-76)

BEGIN FIRST LINE OF TEXT HERE
TYPING GUIDE SHEET
CENTER OF PAGE
TOP OF IMAGE AREA
DROPPED HEAD; BEGIN SECTIONS HERE

CONTENTS

Foreword iii
Abstract iv
Figures vi
Tables viii
Abbreviations and Symbols x
Acknowledgment xiv

1. Introduction 1
2. Conclusions 3
3. Recommendations 4
4. Spatial Variability of Soil Parameters 5
   Sample numbers 8
5. Scaling of Soil Hydraulic Properties 12
   Scaled hydraulic properties 12
   Scaling the soil moisture flow equation 13
6. Infiltration 16
7. Field Drainage--Simplified 23
   Monte Carlo simulation 23
   Taylor series solution 24
   Drainage following uniform sprinkling 26
8. Field Drainage--Non-Linear Analysis 28
   Cyclical water application 31
9. Solute Movement 36
   Theory 36
   Field data 39
   Numerical examples 39
10. Sensitivity 46
   Simple drainage equation--sensitivity 47
   Non-linear drainage--sensitivity 48

References 54
Publications and Papers Associated with Results 57
Appendix
   Finite Difference Program--Flux Specified at Boundary 58

BEGIN LAST LINE OF TEXT
BOTTOM OF IMAGE AREA OUTSIDE DIMENSION FOR TABLES AND ILLUSTRATIONS
3/8"

EPA-287 (Cin.)
(4-76)

BEGIN FIRST LINE OF TEXT HERE
TYPING GUIDE SHEET
CENTER OF PAGE
TOP OF IMAGE AREA
DROPPED HEAD; BEGIN SECTIONS HERE

FIGURES

Number		Page
1	Mean values of J_L expected 95% of the time as a function of size for the 180-cm soil depth. (Values for the variance were taken as 6260, 4.49 and 0.073 for t = 0, 1, and 10 days, respectively.)	11
2	Soil water characteristics data for six depths of Panoche soil: (A) unscaled and (B) scaled.	14
3	Probability plots of α_r and ln α_r calculated from soil water characteristics data for all six depths of Panoche soil.	15
4	Moisture profiles for α = 1.23, 0.873, and 0.618 (75, 50, and 25 percentile values, respectively)	19
5	Intake velocities: A. Scaled intake velocity. B. Real intake velocity. Shaded area denotes 25-75 percentile range. C. Mean and 25-75 percentile ranges for "halved" and "doubled" variance calculations (see text).	20
6	Intake rates for α_r = 1 (deterministic) compared to the mean values (Part A), and effect of initial condition on $\hat{v}_o$ as calculated by three terms of the semi-analytical solution (Part B).	21
7	J_L values for t = 0 through t = 20 days for the 180-cm soil depth. The bars are ranges for the middle 50% of the values at specific times.	25
8	Flux values as a function of time for drainage following uniform sprinkling. Shaded area is for the middle 50% of values	27
9	Mean drainage velocities at the 40-cm (A) and 180-cm (B) depths (solid lines). The 25 and 75 percentiles are shown by dashed lines.	30
10	Moisture profiles at 1, 2, 13, and 24 hours (a, b, c, and d, respectively) into cycle for high frequency irrigation. In each sketch, the three curves from left to right are the 75 percentile, the mean and the 25 percentile values of the scaling coefficient.	34

8-1/2"
BEGIN LAST LINE OF TEXT
BOTTOM OF IMAGE AREA; OUTSIDE DIMENSION FOR TABLES AND ILLUSTRATIONS
3/8"

EPA-287 (Cin.)
(4-78)

BEGIN FIRST LINE OF TEXT HERE
TYPING GUIDE SHEET
CENTER OF PAGE
TOP OF IMAGE AREA
DROPPED HEAD; BEGIN SECTIONS HERE
6-1/2"
BEGIN LAST LINE OF TEXT
BOTTOM OF IMAGE AREA; OUTSIDE DIMENSION FOR TABLES AND ILLUSTRATIONS
3/8"
PAGE NUMBER
EPA-287 (Cin.) (4-76)

Number		Page
11	Values of moisture content during the 24-hour cycle at the surface and the 40-cm depth. The lower, middle and upper curves in each case are for the 75 percentile, the mean and the 25 percentile values of the scaling coefficient, respectively.	35
12	Effect of changing apparent diffusion coefficient D (Parts A and B) and the velocity v (Parts C and D).	38
13	Average relative solute concentration with depth for a step input of salt water after five days.	41
14	Average relative solute concentration with depth for a 7.5-cm pulse of salt water after five days.	41
15	Average solute flux at 60-cm depth for a step input.	42
16	Average solute flux at 60-cm depth for a pulse input	42
17	Average solute flux at 180-cm depth for a step input	43
18	Average solute flux at 180-cm depth for a pulse input.	43
19	Values of $(c/c_o)_{max}$ for v = 44.3 cm/day and random apparent diffusion coefficient (Example 1)	45

BEGIN FIRST LINE OF TEXT HERE
TYPING GUIDE SHEET
CENTER OF PAGE
TOP OF IMAGE AREA
DROPPED HEAD, BEGIN SECTIONS HERE

TABLES

Number		Page
1	Brief Description of Sample Studies on Spatial Variability of Soil Physical Properties.	6
2	Values of Means, Standard Deviations and Coefficients of Variation for Various Soil Properties.	7
3	Summary of Approximate Number of Samples Required to Estimate Mean Values within 10% at 0.05 Significant Level (After Gumaa, 1978)	9
4	Values for λ, χ and ψ from Philip (1969) Analysis. (Also Shown are the Values A, B and C of Equations 18-20)	18
5	Variances, S_f and Coefficients for the Three Chosen Distributions .	22
6	Estimates of the Mean and Variance of ln J_L and J_L for the 180-cm Soil Depth Using Monte Carlo Simulations.	24
7	Values of S_{avg} and Scaled Flux $\hat{v}$ as Functions of X and T for Drainage (the numbers have deliberately not been rounded, see text)	30
8	Choices of Apparent Diffusion Coefficient, D, and Convective Velocity, v, for Monte Carlo Simulations of Mean Solute Distribution and Fluxes	40
9	The Flux J_L, and the Absolute and Relative Sensitivity of J_L with Respect to K_o and α as a Function of Time (for the Simplified Drainage Formula)	48
10	Sensitivity of the Specific Flux, J_L, to K_o and α^* for Panoche. Values are Calculated at K_o = 0.95 cm/day and α^* = 0.04 cm^{-1} (See Equations 75 and 76)	50
11	Sensitivity of Volumetric Moisture Content, Θ, to K_o and α^* for Panoche. Values are Calculated at K_o = 95 cm/day and α^* = 0.04 cm^{-1} (See Equations 75 and 76).	51

BOTTOM OF IMAGE AREA, OUTSIDE DIMENSION FOR TABLES AND ILLUSTRATIONS
BEGIN LAST LINE OF TEXT
3/8"

EPA-287 (Cin.)
(4-76)

BEGIN FIRST LINE OF TEXT HERE
TYPING GUIDE SHEET
CENTER OF PAGE
TOP OF IMAGE AREA
DROPPED HEAD: BEGIN SECTIONS HERE
6-1/2"
9-1/8"
BEGIN LAST LINE OF TEXT
BOTTOM OF IMAGE AREA; OUTSIDE DIMENSION FOR TABLES AND ILLUSTRATIONS
3/8"
1x
PAGE NUMBER
EPA-287 (Cin.)
(4-76)

Number		Page
12	Sensitivity of the Specific Flux, J_L, to K_o for Yolo Soil. Values are Calculated at K_o = 0.0443 cm/hr (see Equations 77 and 78) . .	52
13	Sensitivity of the Volumetric Water Content, θ, to K_o for the Yolo Soil. Values are Calculated at K_o = 0.0443 cm/hr (See Equations 77 and 78).	53

BEGIN FIRST LINE OF TEXT HERE
TYPING GUIDE SHEET
CENTER OF PAGE
TOP OF IMAGE AREA
DROPPED HEAD; BEGIN SECTIONS HERE

LIST OF ABBREVIATIONS AND SYMBOLS

ABBREVIATIONS

erf(u)	-- Error function of argument u.
erfc(u)	-- Complementary error function of argument u.
exp(u)	-- Exponential function of argument u.
E(u)	-- Expected value of argument u.
ln(u)	-- Natural logarithm of argument u.
$N(\mu, \sigma^2)$	-- Normal distribution of mean μ and variance σ^2.

SYMBOLS

A	Integral of λ from S_f to S_i (units $L/T^{1/2}$).
A_j	Coefficient for finite differencing (dimensionless).
B	Integral of χ from S_f to S_i (units L/T).
B_j	Coefficient for finite differencing (dimensionless). (Also coefficient for cyclic irrigation, Equation 52).
C	Integral of ψ from S_f to S_i (units $L/T^{3/2}$).
C_j	Coefficient for finite differencing (dimensionless).
c	Concentration of soil water solute (units unspecified).
c_o	Concentration of water added to the soil profile (units unspecified).
$(c/c_o)_{max}$	Maximum concentration ratio within profile.
D	Apparent diffusion coefficient (units L^2/T). Also soil water diffusivity (units L^2/T). (Also specified limit for estimating sample mean, Equation 1 only).

BEGIN LAST LINE OF TEXT
BOTTOM OF IMAGE AREA; OUTSIDE DIMENSION FOR TABLES AND ILLUSTRATIONS
3/8"
PAGE NUMBER
EPA-287 (Cin.) (4-76)

BEGIN FIRST LINE OF TEXT HERE
TYPING GUIDE SHEET
CENTER OF PAGE
TOP OF IMAGE AREA

D_j^n	Soil water diffusivity at jth space and nth time node (units L^2/T).
D^*	Soil water diffusivity for linearized case (units L^2/T).
f	Darcian velocity at boundary for linearized case (units L/T).
f_o	Constant Darcian velocity at boundary for linearized case (units L/T).
f_∞	Darcian velocity at deep depth for linearized case (units L/T).
H_j	Coefficient for finite differencing (dimensionless).
h	Pressure head (soil water pressure - soil air pressure) (units L).
$\hat{h}$	Scaled pressure head (units L).
$h_{r,i}$	Pressure head at rth site, ith increment (units L).
I	Cumulative intake at surface (units L).
I_o	Initial intake velocity (units L/T).
$\hat{I}$	Scaled cumulative intake (units L).
J_L	Darcian flux (units L/T).
j	Used for space increment in finite differencing.
K	Unsaturated hydraulic conductivity (units L/T).
K_o	Constant used for one of two forms of unsaturated hydraulic conductivity (different units).
K_{sat}	Saturated hydraulic conductivity (units L/T).
K_j^n	Unsaturated K at jth space and nth time node (units L/T).
$\hat{K}$	Scaled unsaturated hydraulic conductivity (units L/T).
k^*	For linearized case $dK/d\Theta$ (units L/T).
L	Depth used for simplified drainage equation (units L).
N	Sample number.
n	Used for time increment in finite differencing.
R	Surface water input (units L/T).

DROPPED HEAD; BEGIN SECTIONS HERE
6-1/2"
9-1/8"
BEGIN LAST LINE OF TEXT
BOTTOM OF IMAGE AREA; OUTSIDE DIMENSION FOR TABLES AND ILLUSTRATIONS
3/8"

EPA-287 (Cin.)
(4-76)

BEGIN FIRST LINE OF TEXT HERE
TYPING GUIDE SHEET
CENTER OF PAGE
TOP OF IMAGE AREA
DROPPED HEAD; BEGIN SECTIONS HERE
BEGIN LAST LINE OF TEXT
BOTTOM OF IMAGE AREA; OUTSIDE DIMENSION FOR TABLES AND ILLUSTRATIONS
6-1/2"
9-1/8"
3/8"
PAGE NUMBER
EPA-287 (Cin.)
(4-76)

S	Degree of saturation Θ/Θ_{sat} (dimensionless).
$S_{A,i}$	Absolute sensitivity of ith variable (units vary).
S_{avg}	Average degree of saturation in profile (dimensionless).
S_f	Final degree of saturation (dimensionless).
S_i	Initial degree of saturation (dimensionless).
$S_{r,i}$	Degree of saturation at rth site, ith increment (dimensionless).
$S_{R,i}$	Relative sensitivity of ith variable (dimensionless).
$S_{R,i}^*$	Relative sensitivity of Equation 72 (dimensionless).
S_j^n	Degree of saturation at jth space and nth time node (dimensionless).
S_∞	Value of degree of saturation for deep depths (dimensionless).
s^2	Estimate of population variance (units vary).
T	Scaled time (units T).
t	Time (units T).
v	Convective velocity, pore water velocity (Darcian velocity in Section 8 only) (units L/T).
v_o	Surface intake velocity (units L/T).
$\hat{v}_o$	Scaled surface intake velocity (units L/T).
$\hat{v}$	Scaled Darcian velocity (units L/T).
X	Scaled depth (units L).
X_o	Scaled depth for which unit gradient specified (units L).
x	Depth in profile (units L).
α	Scaling coefficient (dimensionless). (Alternative use as probability level in Euqation 1 only).
α_r	Scaling coefficient at site r (dimensionless).
α^*	Constant used for specific unsaturated water content (units 1/L).
β	Used in special form of unsaturated K (Equation 77).

BEGIN FIRST LINE OF TEXT HERE
TYPING GUIDE SHEET
CENTER OF PAGE
TOP OF IMAGE AREA
DROPPED HEAD; BEGIN SECTIONS HERE

Δt_{wet}	Time increment for wetting part of cycle (units T).
Δt_{dry}	Time increment for drying part of cycle (units T).
Θ	Volumetric water content (dimensionless).
Θ_o	Volumetric water content at time zero (dimensionless).
Θ_s	Saturated volumetric water content (dimensionless).
Θ_r	Used in special form of soil water characteristic (Equation 78).
λ	First coefficient for infiltration (units $L/T^{1/2}$).
μ	Population mean (units vary).
σ^2	Population variance (units vary).
$\sigma_{\alpha^*}^2$	Population variance for α^* (dimensionless).
$\sigma_{J_L}^2$	Population variance for J_L (units L^2/T^2).
$\sigma_{K_o}^2$	Population variance for K_o (units L^2/T^2).
χ	Second coefficient for infiltration (units L/T).
ψ	Third coefficient for infiltration (units $L/T^{3/2}$).

9-1/8"
BEGIN LAST LINE OF TEXT
BOTTOM OF IMAGE AREA; OUTSIDE DIMENSION FOR TABLES AND ILLUSTRATIONS
3/8"

EPA-287 (Cin.)
(4-76)

TYPING GUIDE SHEET
BEGIN FIRST LINE OF TEXT HERE
CENTER OF PAGE
TOP OF IMAGE AREA
DROPPED HEAD; BEGIN SECTIONS HERE
6-1/2"
9-1/8"
BEGIN LAST LINE OF TEXT
BOTTOM OF IMAGE AREA; OUTSIDE DIMENSION FOR TABLES AND ILLUSTRATIONS
3/8"
PAGE NUMBER
EPA-287 (Cin.) (4-76)

ACKNOWLEDGMENT

The preparation of this report was supported by Grant No. R-804751, U.S. Environmental Protection Agency. The cooperation of Dr. Arthur G. Hornsby, Project Officer, Robert S. Kerr Environmental Research Laboratory, Ada, Oklahoma is gratefully acknowledged.

BEGIN FIRST LINE OF TEXT HERE
TYPING GUIDE SHEET
CENTER OF PAGE
TOP OF IMAGE AREA
DROPPED HEAD: BEGIN SECTIONS HERE

SECTION 1

INTRODUCTION

This two-year study dealt with areal predictions of water and solute fluxes within the soil profile. The project was designed to develop methods to account quantitatively for the inherent variability of soils over a region --such as an irrigated field or larger.

The problems of areal distribution and predictions encompass all aspects of earth sciences. An immediate and obvious connection between soil physical properties and soil maps exists and suggests mutual benefits for an even closer cooperation between classifiers and the other soil scientists. This doesn't apply just to soil physical measurements, but also to any other soil property, e.g., fertility level, chemical activity and distributions of biomass and microbes.

Two very important observations should be made in terms of trends of current research and awareness since the inception of this project: (1) there has been a tremendous increase of interest in variability of soil properties and (2) there has been an equally impressive increase among the American hydrologists with regard to geostatistical techniques which were largely ignored until recently. The two developments are related.

Soil scientists (and farmers) have always recognized that soils are variable. However, the approach, by necessity, has been almost universally deterministic in nature. The procedure has generally been to sample, average the samples, and use the results to make calculations. For example, if a mass flux of salts is needed, the land area is multiplied by the "average" profile result to get total emissions. That such an approach may not give the right answer is stated in elementary works on stochastic processes (e.g. Hammersly and Handscomb, 1964, especially p. 13) and is demonstrated in the case of mean water flux by Warrick et al. (1977b) and in results from this project. In some cases, a choice other than the arithmetic mean may be appropriate; in other cases, no "average" value may be satisfactory to obtain an overall response or integrated estimate. Efforts to adequately assess confidence of results have been generally lacking.

The upsurgence of geostatistics is due primarily to successes by the South Africans (particularly, Krige) and French (particularly, Matheron and associates) regarding estimates and management in mining engineering. The accepted usage of "geostatistics" is strongly entwined with their methods (e.g. Journel and Huijbregts, 1978) including "Kriging". They offer an alternative to some of the conventional statistics. The basic approach is to

BEGIN LAST LINE OF TEXT
BOTTOM OF IMAGE AREA; OUTSIDE DIMENSION FOR TABLES AND ILLUSTRATIONS
3/8"

EPA-287 (Cin.)
(4-76)

BEGIN FIRST LINE OF TEXT HERE
TYPING GUIDE SHEET
CENTER OF PAGE
TOP OF IMAGE AREA
DROPPED HEAD; BEGIN SECTIONS HERE

consider the spatial structure such that samples will be correlated as a function of space with samples from close to each other generally alike compared to samples which were separated by large distances. This is contrasted with an analysis based on independent observations. Embedded in the analysis are stochastical notions, regional averages, best fits and confidence intervals.

The techniques within this project are somewhat intermediate between the deterministic and the geostatistical methods. Ramifications of spatial variability are pursued in terms of water and salt fluxes, primarily by Monte Carlo simulations. Although we were cognizant from the beginning of covariance between closely-spaced locations, the analysis is on the basis of independent samples. The end results are the same for the cases studied, although sampling and confidence intervals can hopefully be obtained more efficiently in the future, by taking advantage of what is known of the spatial structure.

Also in the study are examples of measured variabilities from the literature. Some of the parameters, such as bulk density, are obviously much less variable than others, such as hydraulic conductivity. The consistency of results reported by independent studies is noticeable. In addition, a sensitivity analysis was performed for drainage.

9-1/8"
BEGIN LAST LINE OF TEXT
BOTTOM OF IMAGE AREA, OUTSIDE DIMENSION FOR TABLES AND ILLUSTRATIONS
3/8"

PAGE NUMBER
EPA-287 (Cin.)
(4-76)

BEGIN FIRST LINE OF TEXT HERE
TYPING GUIDE SHEET
CENTER OF PAGE
TOP OF IMAGE AREA
DROPPED HEAD; BEGIN SECTIONS HERE

SECTION 2

CONCLUSIONS

1. Observed variations of soil parameters in the literature were remarkably consistent when more than one source was found. Generally these parameters can be categorized in three classes:

Low variability: (Coefficient of variation less than 20%)
- Bulk density
- Water content at a zero tension

Medium variability: (Coefficient of variation 20-75%)
- Textures (sand, silt or clay)
- Field water content
- Water content at specified tension between 0.1-15 bars.

High variability: (Coefficient of variation greater than 100%)
- Saturated Hydraulic conductivity
- Unsaturated hydraulic conductivity
- Apparent diffusion coefficient
- Pore water velocity
- Electrical conductivity
- Scaling coefficients

2. Scaling techniques offer distinct advantages in terms of economy of calculations. (Also scaling techniques offer advantages in synthesizing large volumes of data.)

3. In simulating movement of salts pulses through profiles under ponded conditions, the "average" depth and concentrations in the profile are considerably different than that described by the average velocity and apparent diffusion coefficient.

4. The Rubin-Steinhardt (1963) model is appropriate for simulating a water flux boundary condition for one-dimensional non-linear flow. (A unit-gradient boundary condition was used for the lower boundary condition.)

5. For simulating cyclic water conditions for a scaled system, higher values of the scaling coefficient correspond to regions where responses are faster but changes were less than for a small scaling coefficient.

BEGIN LAST LINE OF TEXT
BOTTOM OF IMAGE AREA; OUTSIDE DIMENSION FOR TABLES AND ILLUSTRATIONS
3/8"

EPA-287 (Cin.)
(4-76)

BEGIN FIRST LINE OF TEXT HERE
TYPING GUIDE SHEET
CENTER OF PAGE
TOP OF IMAGE AREA
DROPPED HEAD; BEGIN SECTIONS HERE

SECTION 3

RECOMMENDATIONS

1. For future studies, variability of data should always be included along with the mean values. Information regarding observed frequency distributions and/or spatial distributions is also helpful.

2. For future studies, consideration should be given to sensitivity of results to pertinent parameters. Much could be gained by consistently using the relative sensitivity values when wishing to make quantitative comparisons.

3. Basic research is required regarding well-known soil parameters in order to determine optimum sample volume as well as the spacing. Sound, scientific data are practically non-existent, for example, on judging whether a few grams or a metric ton describes a site for a given analysis.

4. Use of "geostatistics" should be pursued in soil science, both in terms of basic descriptions and for integrating results over large areas. To some extent, researchers and practitioners should guard against abandoning proven techniques and being oversold on a "hot" technique, but we are far from utilizing these new methods to their potential.

5. With regard to Monte Carlo simulations, advanced techniques, such as stratification, should be attempted to economize "sample numbers".

BEGIN LAST LINE OF TEXT
BOTTOM OF IMAGE AREA; OUTSIDE DIMENSION FOR TABLES AND ILLUSTRATIONS
3/8"

EPA-287 (Cin.)
(4-76)

BEGIN FIRST LINE OF TEXT HERE
TYPING GUIDE SHEET
CENTER OF PAGE
TOP OF IMAGE AREA
DROPPED HEAD BEGIN SECTIONS HERE

SECTION 4

SPATIAL VARIABILITY OF SOIL PARAMETERS

In this section, data collected by several different groups describing the variability of soil physical parameters are presented. Our goal is to illustrate the type of measurements and studies which have been completed, and not to provide an exhaustive, comprehensive review. We emphasize quantitative determination of soil physical parameters. After presenting the data, we will briefly discuss sampling size determination and expected "accuracy." Ramifications of the variability on specific fluxes in soil are left to later chapters.

6-1/2"

Of the studies listed in Table 1, that of Nielsen et al. (1973) is the most comprehensive. In our later work, the variability of unsaturated hydraulic conductivity, of the apparent diffusion coefficient and of the "scaling" coefficients is based upon their results. The experiments were conducted at the University of California, West Side Field Station near Fresno, California, on Panoche loam. The Panoche soils have generally uniform profiles, but a wide range of textures. Twenty plots, each 6.5 x 6.5 m, were randomly established over the 150-hectare farm. Tensiometers and sampling cups were situated in the center of the plots, which were then flooded, saturated and allowed to drain. Values of soil water tension and soil water solute concentration were collected over an extensive period. For each site, two pits were dug and cores were collected in triplicate from opposite sides (i.e. 6 cores x 20 sites = 120 cores for each depth). Soil water characteristics were run for every core and results were "averaged" for each depth at each site.

Of the other studies, that of Gumaa (1978) is used the most extensively. Samples were collected from 16 hectare fields on a square 50 m grid. Bulk samples were collected from 56 sampling sites at five depths at approximately two days after a heavy (300 mm) irrigation. In two fields, this was repeated again in four weeks. Sixty-four cores were taken from two fields, with only ten from the third field. The cores were used to determine saturated hydraulic conductivity and bulk density.

In examining the various experimental results, we are interested in descriptive parameters (e.g. mean and variance or coefficient of variation), type of distribution, homogeneities and correlations both with space and between parameters. Here we will address primarily the coefficient of variations and observed distribution types.

BOTTOM OF IMAGE AREA; OUTSIDE DIMENSION FOR TABLES AND ILLUSTRATIONS
BEGIN LAST LINE OF TEXT

Sample means, standard deviation and coefficient of variation were chosen for several parameters and are shown in Table 2. Three groups were

3/8"

EPA-287 (Cin.)
(4-76)

BEGIN FIRST LINE OF TEXT HERE
TYPING GUIDE SHEET
CENTER OF PAGE
TOP OF IMAGE AREA
DROPPED HEAD; BEGIN SECTIONS HERE

TABLE 1. BRIEF DESCRIPTION OF SAMPLE STUDIES ON SPATIAL VARIABILITY ON SOIL PHYSICAL PROPERTIES

Source(s)	Soil Series or Location	Number of Locations	Soil Depths	Parameters (May be partial listing)	Comments
1. Nielsen et al. (1973); Biggar and Nielsen (1976); Warrick et al.(1977a,b)	Panoche (California)	20	30,60,90, 120,150, 180 cm	Particle size, soil water characteristics, 15-bar water, bulk density, water stored in profile, steady infiltration rate, unsaturated K, saturated K, water distribution in profile, soil water flux, apparent diffusion coefficient.	Sites randomly located within 150 ha
2. Coelho (1974), Warrick et al. (1977a)	Pima (Arizona)	36	30,60,90, 120,150	Particle size, soil water characteristics, 15-bar water, bulk density, saturated K, scaling coefficient.	Randomly chosen nested design within 87 ha
3. Keisling (1974)	Teller (Oklahoma)	8	15,30,45, 60,75,90, 120,150	Particle size, bulk density, soil water characteristics, 15-bar water, unsaturated K.	Three sites within 0.15 km, all within 7.2 km.
4. Gumaa (1978)	Eight series in 3 fields (Arizona)	167	30,60,90, 120,150cm	Particle size, soil water characteristics, 15-bar water, bulk density, saturated K, in situ field capacity.	3 fields each of 16 hectares, 2 were contiguous.
5. Wagenet and Jurinak(1978)	Mancos Shale (Utah)	35	0-2.5,2.5-7.5,7.5-15	Electrical conductivity of saturation and 1:1 extract	Within 777 km^2 area
6. Blyth and Maclecd(1978)	Six forests in Scotland	65	Surface & about 20cm	pH, total N, total P, acetic acid titratable P,K, Ca, Mg	Each plot 0.01 hectare or 1 hectare
7. Cameron (1978)	Bainsville (Saskatchewan)	5	0-15,15-30 30-45,45-60,60-90, 90-120	Particle size, soil water characteristics, 15-bar water, bulk density, particle density, unsaturated K	225 m^2
8. Cassel and Bauer (1975)	Three soils (N. Dakota)	408	4 or 5 depths to 150 cm	Bulk density, 15-bar water	1.3 ha for first area and 3 blocks of 0.5 ha within 150 m for each of the other two.
9. Carvallo et al. (1976)	Maddock (N. Dakota)	5 plots	15,30,45, 60,90,120, 150	Particle size, bulk density, soil water characteristics, unsaturated K.	0.01 hectare
10. Van de Pol et al.(1977)	Plant Sci. Res. Center (N. Mexico)	3 sites within plot	7 or 8 depths to 150 cm	Unsaturated K, apparent diffusion coefficient	8 m x 8 m
11. Webster (1977)	A gilgai soil (New S. Wales)	Transect 375 locations	0 to 10 30 to 40 80 to 90cm	pH, electrical conductivity, chloride, bulk density and others	4 m intervals for 15 km. Shows spectra.
12. Willardson and Hurst (1965)	Gila-Yinton (California)	330 values	1 to 90 1 to 150 1 to 210cm	Saturated K	Data from Soil Conservation Service. Also other Imperial Valley and Australian soils.

BEGIN LAST LINE OF TEXT
3/8"
EPA-287 (Cin.) (4-76)

PAGE NUMBER
BOTTOM OF IMAGE AREA; OUTSIDE DIMENSION FOR TABLES AND ILLUSTRATIONS

BEGIN LAST LINE OF TEXT
DROPPED HEAD; BEGIN SECTION IS HERE
BEGIN FIRST LINE OF TEXT HERE
EPA-287 (Cin.) (4-76)
3/8"
PAGE NUMBER
TYPING GUIDE SHEET
CENTER OF PAGE
BOTTOM OF IMAGE AREA; OUTSIDE DIMENSION FOR TABLES AND ILLUSTRATIONS
TOP OF IMAGE AREA

TABLE 2. VALUES OF MEANS, STANDARD DEVIATIONS AND COEFFICIENTS OF VARIATION FOR VARIOUS SOIL PROPERTIES

Parameter	Mean	Standard Deviation	Coefficient of Variation (%)	Source (See Table 1)
Low Variation				
Bulk density (g/cm^3)	1.3	0.09	7.0	Gumaa, Field 1, 5 combined depths on 64 cores
	1.4	0.095	7.0	Nielsen et al. combined data for all depths
	1.5	0.11	7.8	Cassel and Bauer, 30-60 cm depth, Oakes soil
Water content (%) at zero tension (cm^3/cm^3)	40/45	4.5/4.8	11/10	Nielsen et al., 30-cm depth and combined depths
	47	4.8	10	Cameron, 15-30 cm depth
Medium Variation				
Sand/silt/clay (%)	53/28/19	15/1.1/6.8	28/32/36	Gumaa, Field 1 at 30 cm
	59/29/12	22/18/6.4	32/60/54	Gumaa, Field 1, 5 combined depths
	26/27/47	11/6/8	43/23/18	Nielsen et al., 30-45 cm depths
	24/30/45	14/8/10	55/27/23	Nielsen et al., 12 combined depths
Water content (%) 0.1/15 bar (g/g)	27/9.5	5.4/3.1	20/33	Gumaa, Field 1, 30 cm depth
0.2 bar (cm^3/cm^3)	23.2/7.5	9.2/3.8	40/50	Gumaa, Field 1, 5 combined depths
	32	5.4	17	Nielsen et al., 30 cm depths
	32	7.7	24	Nielsen et al., combined depths
2.2 bar (cm^3/cm^3)	34	4.1	12	Cameron, 15-30 cm depth
15 bar (g/g)	4.5	1.4	31	Cassel, 30-60 cm depth, Oakes
High Variation				
Saturated hydraulic conductivity (cm/hr)	14	26	190	Gumaa, Field 1, 5 combined depths and 64 cores
Log of saturated hydraulic conductivity	0.3	0.5	57	" " " " " " " "
Saturated hydraulic conductivity(cm/day)	20	22	110	Nielsen et al., combined depths
Log of saturated hydraulic conductivity as inches/hr	-0.84	0.72	86	Willardson and Hurst (330 values)
Unsaturated hydraulic conductivity (cm/day)(90 and 60% of saturation)	0.63/ 0.0026	1.75/0.011	280/440	Nielsen et al., 30 cm depth
	4.9/0.12	8.1/0.47	170/400	Nielsen et al., combined depths
Apparent diffusion (cm^2/day)	370	$(2.4)(10)^6$	$(6.5)(10)^6$	Biggar and Nielsen, all depths
Pore water velocity (cm/day)(from water and from solute)	44/40	7300/4400	$(1.7)(10)^4$/ $(1.1)(10)^4$	Biggar and Nielsen, all depths
Electrical conductivity in µmho/cm for 1:1 extract and saturation extract	3200/3100	8100/3900	250/130	Wagenet and Jurinak, 7.5-15 cm depth
Log of scaling coefficient (no units)	-0.136	0.512	380	Warrick et al., Panoche combined depths.

BEGIN FIRST LINE OF TEXT HERE
TYPING GUIDE SHEET
CENTER OF PAGE
TOP OF IMAGE AREA
DROPPED HEAD: BEGIN SECTIONS HERE

selected as "low", "medium" and "high" variability. We imply these particular parameters may generally be expected to fall in the same relative categories under most conditions. Of course, the values are certainly not universal, but rather only illustrative. We might expect, for example, a very strongly developed profile to show higher variabilities when not grouped by depths, but quite likely the coefficient of variation would be smaller for any group of samples chosen from the "low" category, e.g. as for the bulk density, than for a parameter from the "high" variability group, e.g. unsaturated hydraulic conductivity. The measurement error can also be a major factor which we do not try to separate from the "true" value.

Bulk density and saturated water content consistently had the lowest amount of variation of the parameters studied. For the Cassel and Bauer (1975), Nielsen et al. (1973), and Gumaa (1978) results (see Table 1), the coefficients of variation were on the order of 7-8 percent. Similarly, the water retained at zero pressure (i.e. approximately saturated) was on the order of 10 percent, both by Cameron (1978) and by Nielsen et al. (1973). These distributions also tend towards normality. For example, Nielsen et al. (1973) plot the sample frequency distribution (their Figure 6) and find close agreement with an actual normal curve.

The highest variations are for the saturated and unsaturated hydraulic conductivities, apparent diffusion coefficient, pore water velocities, and scaling coefficients. Each of these parameters has a highly skewed distribution pattern and tends to be more closely approximated by a log normal distribution than a normal distribution (cf. Nielsen et al. (1973), Figure 16; Biggar and Nielsen (1976), Figures 3 and 5; Coelho (1974), Figure 10). For logarithmically transformed values, Willardson and Hurst (1965) give a coefficient of variation of 86 percent. Gumaa (1978), and Nielsen et al. (1973) give values for saturated conductivities from about 90 to 180 percent. The variation for unsaturated conductivities is on the order of 200-400 percent. Estimates for the pore water velocities and apparent diffusion coefficient are much larger, having values of 10^{4}-10^{6}. These latter variables are very difficult to determine experimentally.

The degree of variability of the other parameters listed in Table 2 are intermediate, with a coefficient of variation of between 10 and 100%. Values for primary textures show a range of 12-54 percent. Nielsen et al.'s values are considerably lower than Gumaa's, probably because the soil studied by the latter were more stratified. Water content values tend to show larger coefficients for higher tensions. Nielsen et al. (1973) showed 17 and 24 percent variation at 0.2 bar compared to 10 and 11 percent for the zero tension. Gumaa (1978) showed 20 and 40 percent for 0.1 bar corresponding to 33 and 50 percent for 15 bar. Wagenet and Jurinak (1978) showed values for the log of electrical conductivity of about 20% for both a 1:1 extract and a saturated extract. Their sample distribution had a definite tendency to be log normal.

SAMPLE NUMBERS

The number of samples necessary to approximate the mean can be calculated using Petersen and Calvin (1965, especially p. 59)

BEGIN LAST LINE OF TEXT
BOTTOM OF IMAGE AREA; OUTSIDE DIMENSION FOR TABLES AND ILLUSTRATIONS
3/8"

EPA-287 (Cin.)
(4-76)

BEGIN FIRST LINE OF TEXT HERE
TYPING GUIDE SHEET
CENTER OF PAGE
TOP OF IMAGE AREA
DROPPED HEAD: BEGIN SECTIONS HERE
6-1/2"
9-1/8"

$$N = t_{\alpha}^2 s^2 / d^2 \quad (1)$$

where N is the number of samples, t_{α} is the "Student's t" with n-1 degrees of freedom at the probability level α, s is the standard deviation and d a specified limit. Assumptions are that the samples are independent and that the central limit theorem applies (i.e. the estimate of the mean is from a normally distributed population regardless of the underlying population distribution). For a corresponding formula for a stratified sample, see Petersen and Calvin (1965, especially p. 67).

TABLE 3. SUMMARY OF APPROXIMATE NUMBER OF SAMPLES REQUIRED TO ESTIMATE MEAN VALUES WITHIN 10% AT 0.05 SIGNIFICANT LEVEL (AFTER GUMAA, 1978)

Parameters	Field	Soil Depth, cm 30	60	90	120	150
Low Variation						
Bulk density	1	1	1	1	1	1
	2	1	1	1	1	1
	3	1	1	1	1	1
Medium Variation						
In situ field capacity	1	10	28	24	47	2
	2	12	23	61	49	75
	3	10	9	15	10	24
In situ available water capacity	1	21	43	35	55	45
	2	55	36	110	78	116
	3	47	31	33	30	45
15 bars	1	20	55	33	57	47
	2	25	78	68	57	125
	3	23	19	31	35	30
% clay	1	25	49	33	51	47
	2	28	91	104	36	110
	3	20	18	24	36	36
% silt	1	20	57	66	122	71
	2	16	61	88	83	104
	3	8	20	47	28	40
% sand	1	15	28	13	27	43
	2	19	16	21	23	47
	3	1	1	3	2	3
High Variation						
K_{sat}	1	110	150	362	635	155
	2	119	49	155	102	560

Table 3 summarizes the approximate number of samples required to estimate mean values within 10% at the 0.05 significance level. The low coefficients of variation translate into very small sample numbers, e.g. as

BEGIN LAST LINE OF TEXT HERE
BOTTOM OF IMAGE AREA; OUTSIDE DIMENSION FOR TABLES AND ILLUSTRATIONS
3/8"

PAGE NUMBER
EPA-287 (Cin.) (4-76)

BEGIN FIRST LINE OF TEXT HERE
TYPING GUIDE SHEET
CENTER OF PAGE
TOP OF IMAGE AREA

one for all of the bulk densities. In the same manner, high variations result in large numbers, for example, several hundred samples in the case of the hydraulic conductivities.

DROPPED HEAD: BEGIN SECTIONS HERE

Another way of addressing the same basic problem is to express confidence limits of the estimate of the mean as a function of sample numbers. Figure 1 shows results by Warrick et al. (1977b) showing the mean value of water flux J_L at 180 cm expected 95% of the time as a function of sample size at t = 0, 1 and 10 days. For small sample numbers, the band is wide, for large sample numbers the band narrows. For small n, the limits are imprecise, just as Equation 1 is invalid for small n. The range for flux estimates tend to be fairly wide. For example, for t = 0 samples of 100 and 50 would give estimates of J_L only within 16 and 22 cm/day, respectively. Similar plots are given by Willardson and Hurst (1965) and by Wagenet and Jurinak (1978, especially Figure 3) for saturated hydraulic conductivity and electrical conductivity, respectively.

6-1/2"
9-1/8"
BEGIN LAST LINE OF TEXT
BOTTOM OF IMAGE AREA OUTSIDE DIMENSION FOR TABLES AND ILLUSTRATIONS
3/8"

PAGE NUMBER
EPA-287 (Cin.)
(4-76)

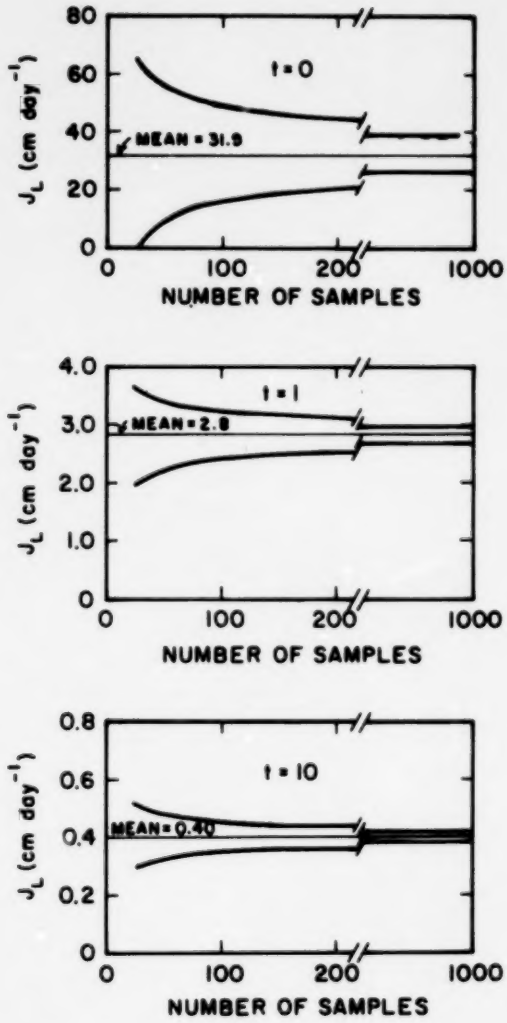

Figure 1. Mean values of J_L expected 95% of the time as a function of sample size for the 180-cm soil depth. (Values for the variance were taken as 6260, 4.49 and 0.073 for t = 0, 1, and 10 days, respectively.)

BEGIN FIRST LINE OF TEXT HERE
TYPING GUIDE SHEET
CENTER OF PAGE
TOP OF IMAGE AREA
DROPPED HEAD: BEGIN SECTIONS HERE

SECTION 5

SCALING OF SOIL HYDRAULIC PROPERTIES

The concept of scaling the hydraulic properties of soils was introduced by E.E. Miller and R.D. Miller (1955) and R.D. Miller and E.E. Miller (1955). Other contributions to the theory of scaling include the works of E.E. Miller and R.D. Miller (1956), Klute and Wilkinson (1958), Wilkinson and Klute (1959), Elrick et al. (1959) and Philip (1967). Warrick et al. (1977a) and Simmons et al. (1980) used the concept to coalesce the soil water characteristics and hydraulic conductivity data.

One of the assumptions is that the internal geometry for similar media differs only by the characteristic size, i.e. each medium is a "blown up" or "scaled-down" version of every other. An immediate consequence of the assumption is that the porosity of every similar sample is the same. Although this assumption is never satisfied exactly, we proceed as if it were and choose the scaling factors on a best fit basis. This is somewhat analogous to linear or nonlinear regression, although, conceptually, we attribute the lack of fit more to physical differences and less to measurement error than do many statistical models.

SCALED HYDRAULIC PROPERTIES

For similar media the pressure head, h_r, at a given moisture content is related to an average pressure head, $\hat{h}$, by

$$h_r = \hat{h}/\alpha_r \qquad (2)$$

where α_r is the scaling coefficient. The corresponding relationship for the hydraulic conductivity, K_r, is

$$K_r = \alpha_r^2 \hat{K} \qquad (3)$$

with $\hat{K}$ an average conductivity at any given moisture content. Thus, $\hat{h}$ and $\hat{K}$ are functions of moisture content and are related to the real h and K at any specific site in the similar media by the scaling coefficient α_r characterizing that particular site.

For the Pima (from Arizona), Panoche (from California) and Teller (from Oklahoma) soils, Warrick et al. (1977a) evaluated the best-fitting $\hat{h}$ as a function of the degree of saturation

BEGIN LAST LINE OF TEXT
BOTTOM OF IMAGE AREA; OUTSIDE DIMENSION FOR TABLES AND ILLUSTRATIONS
3/8"

EPA-287 (Cin.)
(4-76)

BEGIN FIRST LINE OF TEXT HERE
TYPING GUIDE SHEET
CENTER OF PAGE
TOP OF IMAGE AREA

$$S = \theta/\theta_s \quad (4)$$

with θ_s the saturated water content. Although use of S rather than θ does not change the physical system to meet the assumption of a constant θ_s, at least the S values are normalized and everywhere have a maximum of one. Figure 2 shows the results using the pressure head data of the Panoche. The unscaled values are presented in Figure 2A and include seven pressure increments for 20 sites and six depths (giving 840 data points). The scaled heads shown in Figure 2B are the "best" fitting set of 120 α values. The values depend on the particular form of h which is shown, as well as the constraint that the mean of the α value is unity. The fitted equation is

$$\hat{h} = -6020[0.206 - S + 214\ S^2 - 2.04\ S^3 + 0.69\ S^4]/S \quad (5)$$

and reduces the sum of squares by 80% over the same form of equation for the non-scaled data. The α distribution is displayed graphically as Figure 3, as a plot of the cumulative probability versus α_r. A straight line for the α_r would indicate a normal distribution; or a straight line for ln α_r would indicate a log normal distribution. Although there are considerable outliers, we judge the distribution to be approximately log normal where the mean and variance of ln α_r are -0.136 and 0.512, respectively.

For the other soils, they also found the set of α_r to be approximately log normally distributed. For the Panoche soil, they solved for K to give another set of α_r on a best-fitting basis where

$$\ln\hat{K} = -23.3 + 75\ S - 103\ S^2 + 55.7\ S^3 \quad (6)$$

SCALING THE SOIL MOISTURE FLOW EQUATION

The non-linear moisture flow equation for one-dimensional flow with gravity is

$$\partial\theta/\partial t = \partial(D\ \partial\theta/\partial x)/\partial x - \partial K/\partial x \quad (7)$$

We define scaled time, depth and diffusivity by

$$T = (\alpha_r^3/\theta_s)t \quad (8)$$

$$X = \alpha_r x \quad (9)$$

$$\hat{D} = \hat{K}(d\hat{h}/dS) \quad (10)$$

Use of equations 2, 3, 4, 8, 9, and 10 in 7 gives the reduced form

$$\partial S/\partial T = \partial(\hat{D}\ \partial S/\partial X)/\partial X - \partial\hat{K}/\partial X \quad (11)$$

Equation 11 can be solved by any numerical or semi-analytical method for the appropriate boundary and initial conditions. In the next section, we

BOTTOM OF IMAGE AREA; OUTSIDE DIMENSION FOR TABLES AND ILLUSTRATIONS
BEGIN LAST LINE OF TEXT
3/8"

EPA-287 (Cin.)
(4-76)

TYPING GUIDE SHEET
BEGIN FIRST LINE OF TEXT HERE
CENTER OF PAGE
TOP OF IMAGE AREA
DROPPED HEAD: BEGIN SECTIONS HERE

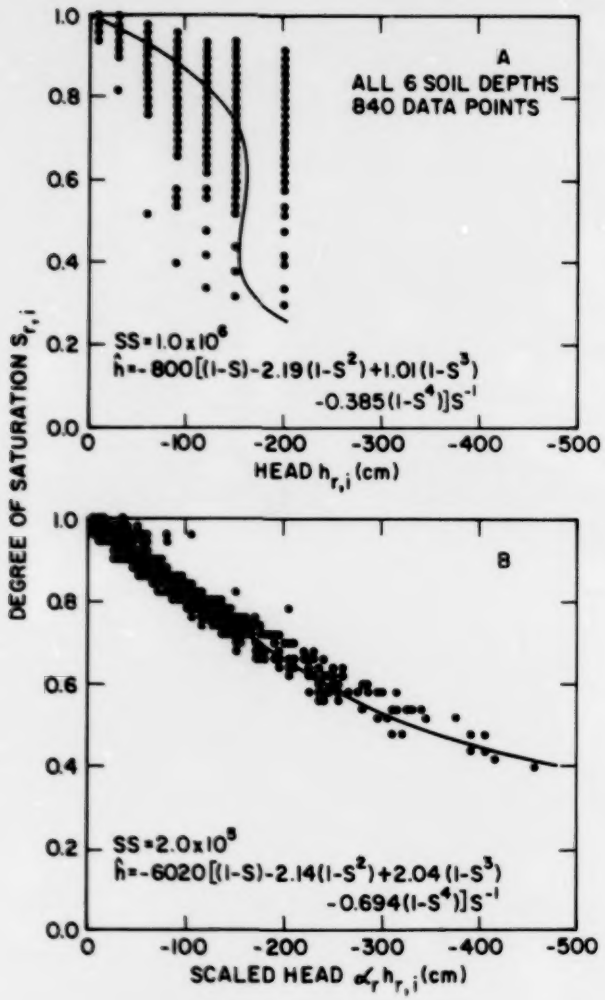

Figure 2. Soil water characteristics data for six depths of Panoche soil: (A) unscaled and (B) scaled.

BEGIN LAST LINE OF TEXT
BOTTOM OF IMAGE AREA; OUTSIDE DIMENSION FOR TABLES AND ILLUSTRATIONS
3/8"

EPA-287 (Cin.)
(4-76)

BEGIN FIRST LINE OF TEXT HERE
TYPING GUIDE SHEET
CENTER OF PAGE
TOP OF IMAGE AREA
DROPPED HEAD BEGIN SECTIONS HERE

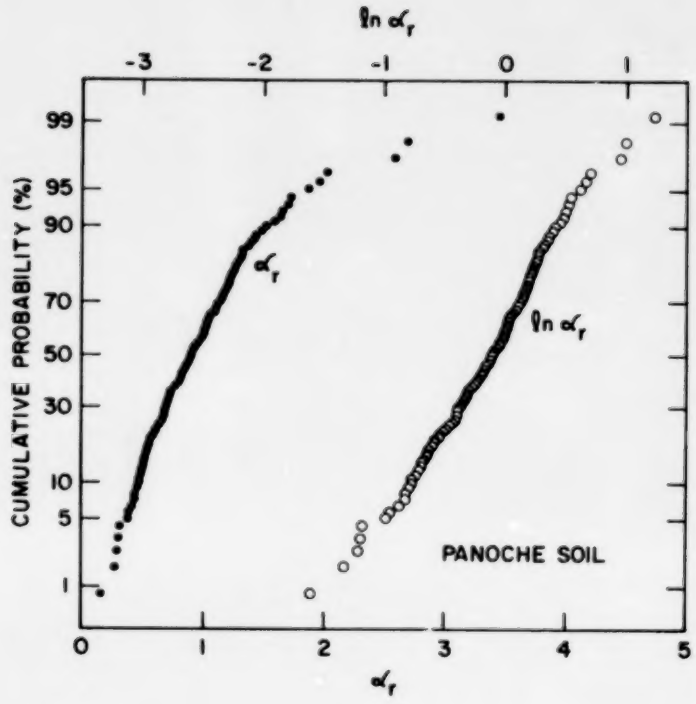

Figure 3. Probability plots of α_r and ln α_r calculated from soil water characteristics data for all six depths of Panoche soil.

will examine infiltration, using the semi-analytical solution of Philip (1969). In still later sections, we consider drainage and cyclic water applications.

BEGIN LAST LINE OF TEXT
BOTTOM OF IMAGE AREA. OUTSIDE DIMENSION FOR TABLES AND ILLUSTRATIONS
3/8"

EPA-287 (Cin.)
(4-76)

BEGIN FIRST LINE OF TEXT HERE
TYPING GUIDE SHEET
CENTER OF PAGE
TOP OF IMAGE AREA
DROPPED HEAD; BEGIN SECTIONS HERE

SECTION 6

INFILTRATION

We assume an initially dry soil with degree of saturation

$$S(X,0) = S_i \tag{12}$$

The surface is assumed to be brought to a constant moisture level

$$S(0,T) = S_f \tag{13}$$

after time zero. The solution to the moisture flow equation (Eq. 11) subject to Equations 12 and 13 is by Philip (1969)

$$X = \lambda(S)T^{1/2} + \chi(S)T + \psi(S)T^{3/2} + \ldots \tag{14}$$

where $\lambda(S)$, $\chi(S)$, and $\psi(S)$ and any additional terms in the series are determined after Philip (1969) or as outlined in detail in Kirkham and Powers (1972).

The cumulative intake, I, is found as the change in storage plus the integrated deep flow rate

$$I = \int_{\theta_i}^{\theta_f} x\,d\theta + K_i t \tag{15}$$

with subscripts "i" and "f", referring to initial and final values of water content. Choosing the first three terms of the series solution Equation 14, gives an intake I of

$$I = (\theta_s/\alpha_r)\,\hat{I} \tag{16}$$

where the scaled intake $\hat{I}$ is

$$\hat{I} = AT^{1/2} + BT + CT^{3/2} \tag{17}$$

with

$$A = \int_{S_i}^{S_f} \lambda(S)\,dS \tag{18}$$

$$B = \int_{S_i}^{S_f} \chi(S)\,dS + \hat{K}(S_i) \tag{19}$$

BEGIN LAST LINE OF TEXT
BOTTOM OF IMAGE AREA; OUTSIDE DIMENSION FOR TABLES AND ILLUSTRATIONS
3/8"

EPA-287 (Cin.)
(4-76)

BEGIN FIRST LINE OF TEXT HERE
TYPING GUIDE SHEET
CENTER OF PAGE
TOP OF IMAGE AREA
DROPPED HEAD; BEGIN SECTIONS HERE

$$C = \int_{S_i}^{S_f} \psi(S)ds \tag{20}$$

The surface intake rate, v_o, is

$$v_o = dI/dt \tag{21}$$

or

$$v_o = \alpha_r^2 \hat{v}_o \tag{22}$$

with the scaled surface intake rate, $\hat{v}_o$, as

$$\hat{v}_o = d\hat{I}/dT = (1/2)AT^{-1/2} + B + (3/2)CT^{1/2} \tag{23}$$

Calculations were made using $S_i = 0$ and S_f chosen in order to match the overall steady intake rate of 14.6 cm/day found in the original field experiment of Nielsen et al. (1973, esp. Figure 1). Thus we solve for S_f by first setting the expected value of $K_r(S_f)$ equal to the overall steady intake rate

6-1/2"

$$E[K_r(S_f)] = 14.6$$

or by Equation 2

$$E(\alpha_r^2)\hat{K}(S_f) = 14.6$$

9-1/8"

The $E(\alpha_r^2)$ is evaluated using the general relationship

$$E(u^n) = \exp(n\mu + n^2\sigma^2/2) \tag{24}$$

where ln u is normally distributed with mean μ and variance σ^2. Thus we have

$$\hat{K}(S_f) = 14.6/\exp(2\mu + 2\sigma^2) \tag{25}$$

where μ and σ^2 are the mean and variance of ln α_r.

Calculations were performed following Philip (1969) with 40 increments and $\theta_s = 0.45$. The assumed values of μ and σ are -0.136 and 0.512, respectively, as estimated for pressure head data (Warrick et al., 1977a). By Equations 6 and 25, the time limiting degree of saturation is $S_f = 0.939$. Values of $\lambda(S)$, $\chi(S)$ and $\psi(S)$ are given in Table 4 along with values of A, B, and C needed for finding surface intake rates. (The computer algorithm was first tested successfully against results in Table 2 of Philip (1957) and Table 4 of Haverkamp et al. (1977).)

Water content (degree of saturation) profiles for Panoche loam are presented in Figure 4 for $\alpha = 1.23$, 0.873, and 0.618. The three different cases are each derived from the single set of λ, χ, and ψ values of Table 4. The differences lie only in the scaling factor α. The largest ($\alpha = 1.23$) corresponds to the 75 percentile of the distribution, i.e. 25% of the values are higher and 75% are lower. The intermediate value is the median ($\alpha = 0.873$) and the smallest is ($\alpha = 0.618$) the 25 percentile, i.e. 25% of the values are

BEGIN LAST LINE OF TEXT
BOTTOM OF IMAGE AREA; OUTSIDE DIMENSION FOR TABLES AND ILLUSTRATIONS
3/8"

PAGE NUMBER
EPA-287 (Cin.) (4-76)

BEGIN FIRST LINE OF TEXT HERE
TYPING GUIDE SHEET
CENTER OF PAGE
TOP OF IMAGE AREA
DROPPED HEAD; BEGIN SECTIONS HERE

TABLE 4. VALUES FOR λ, χ AND ψ FROM PHILIP (1969) ANALYSIS. (ALSO SHOWN ARE THE VALUES A, B AND C OF EQUATIONS 18-20)

S	λ	χ	ψ
0.939	0.0	0.0	0.0
0.867	18.4	4.92	0.778
0.798	22.8	4.15	0.607
0.728	24.2	3.79	0.592
0.657	24.8	3.63	0.591
0.587	25.1	3.55	0.591
0.517	25.3	3.50	0.592
0.446	25.5	3.47	0.592
0.376	25.5	3.45	0.592
0.305	25.6	3.44	0.592
0.235	25.6	3.43	0.592
0.164	25.6	3.43	0.592
0.0939	25.6	3.43	0.592
0.0235	25.6	3.43	0.592
0.0	∞	3.43	0.592
	A = 22.4	B = 3.42	C = 0.584

lower and 75% higher. The procedure for plotting a point was to first calculate the scaled T value from Equation 8 and then find X by Equation 14, using Table 4. Lastly, the corresponding real depth, x, was found by Equation 9.

The large value of α corresponds to a high conductivity region. The large time surface intake is by Equation 3 ($K = \alpha^2 \hat{K}$ or 17.2 cm/day for S_f = 0.939). Similarly, the other plots are for slower intakes, namely 8.64 and 4.33 cm/day. These differences are noticeable in that the large α results in a faster moving water front.

The scaled intake rate $\hat{v}_0$ is plotted as Figure 5. For large times it must be consistent with the physical limiting intake rate, $\hat{v}_0 = 11.37$ by Equation 22. As is well known, the series from the solution of Equation 14 diverges for large times. Thus, Figure 5A was found using Equation 23 for small times and the limiting value of 11.37 for large times (see next paragraph).

The mean value of v_0 is plotted as the solid line in Figure 5B. A Monte

BEGIN LAST LINE OF TEXT
BOTTOM OF IMAGE AREA; OUTSIDE DIMENSION FOR TABLES AND ILLUSTRATIONS
3/8"

EPA-287 (Cin.)
(4-76)

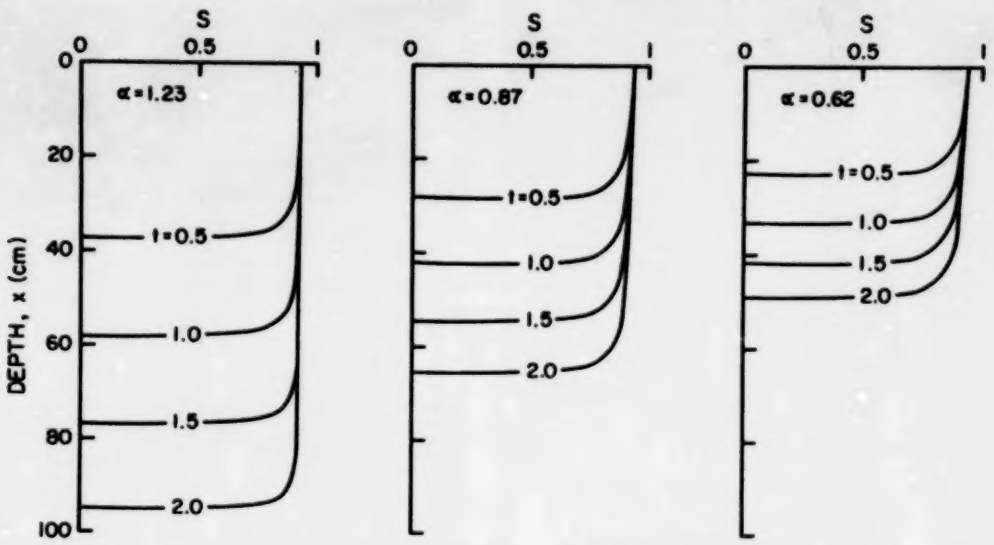

Figure 4. Moisture profiles for α = 1.23, 0.873, and 0.618 (75, 50, and 25 percentile values, respectively).

Carlo simulation was performed as follows for a specified real time t:

(a) A random value of ln α_r was selected from an assumed normal distribution with mean of -0.136 and standard deviation of 0.512.

(b) The scaled time, T, was found by Equation 8.

(c) The dimensionless time was compared to the T_{min} for which the first three terms of Equation 14 give a minimum. If T is greater than this value, v_o is set equal to the large time rate $\alpha_r^2 \hat{v}_o = 11.37\ \alpha_r^2$. If T is less than the time for the minimum to occur, then v_o is set equal to the algebraic value or the limiting value, whichever is greater.

(d) Steps (a)-(c) are repeated and the sample mean and variance are found.

The solid line of Figure 5B is for a sample of 1000 (i.e., each real time was used with 1000 values of α_r) and approaches the 14.6 cm/day as required for large times. Also shown by the shaded area is the limiting range between 25 and 75 percentiles. Twenty-five percent of the true v_o will be above the shaded area and 25 percent will be below. Note the mean value is in the upper range.

BEGIN FIRST LINE OF TEXT HERE
TYPING GUIDE SHEET
CENTER OF PAGE
TOP OF IMAGE AREA
DROPPED HEAD: BEGIN SECTIONS HERE

The mean intake rate can be found algebraically when the series of Equation 23 is valid, i.e. for small times. By Equation 24 we find

$$E(v_o) = E[A/2(\alpha_r\theta_s/t)^{1/2} + \alpha_r^2 B + (3C/2)\alpha^{7/2}(t/\theta_s)^{1/2}] \quad (26)$$

or

$$E(v_o) = (A/2)\exp[\mu/2 + \sigma^2/8](\theta_s/t)^{1/2} + B\exp[2(\mu + \sigma^2)] + (3C/2)\exp[(7/2)\mu + (49/8)\sigma^2](t/\theta_s)^{1/2}, \text{ small } t \quad (27)$$

The result is shown in Figure 5B as the "analytical" points. For t less than two days, the values are the same as for the Monte Carlo simulation. However, for larger times the analytical result starts to diverge and is no longer valid.

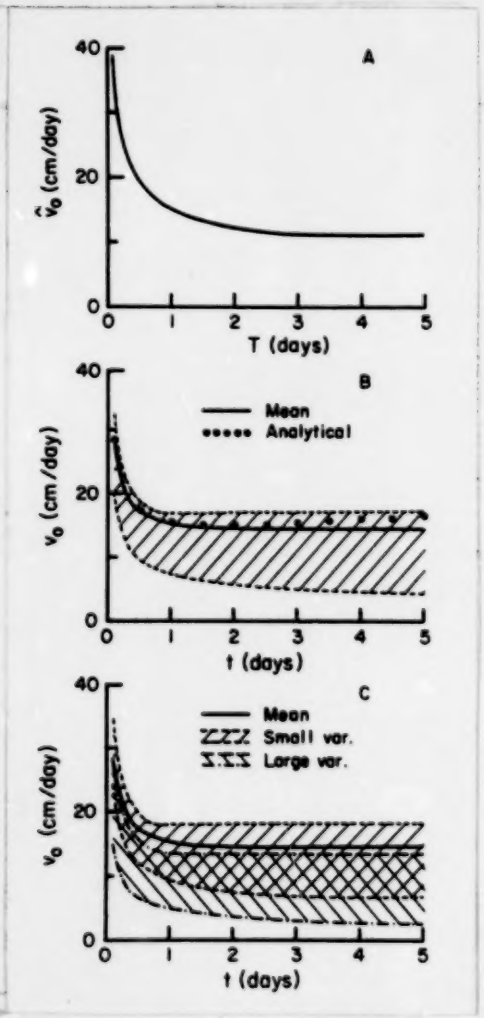

For a deterministic value to compare favorably with the Monte Carlo results, it is necessary to increase S_f at the surface boundary so as to give the correct large time intake value. Thus, we take $\alpha_r = 1$ and choose $S_f = 0.948$ in order to match the steady intake rate of 14.63 cm/day by Equation 3. The result is the "dashed" curve of Figure 6A which is compared to the mean value from the Monte Carlo results of Figure 2B. For small times, there is a slight discrepancy, but for large times they give the chosen identical results.

Effects of varying initial conditions are demonstrated in Figure 6B.

Figure 5. Intake velocities: A. Scaled intake velocity. B. Real intake velocity. Shaded area denotes 25-75 percentile range. C. Mean and 25-75 percentile ranges for "halved" and "doubled" variance calculations (see text).

BEGIN LAST LINE OF TEXT
BOTTOM OF IMAGE AREA; OUTSIDE DIMENSION FOR TABLES AND ILLUSTRATIONS
3/8"

EPA-287 (Cin.) (4-76)

BEGIN FIRST LINE OF TEXT HERE
TYPING GUIDE SHEET
CENTER OF PAGE
TOP OF IMAGE AREA
DROPPED HEAD; BEGIN SECTIONS HERE

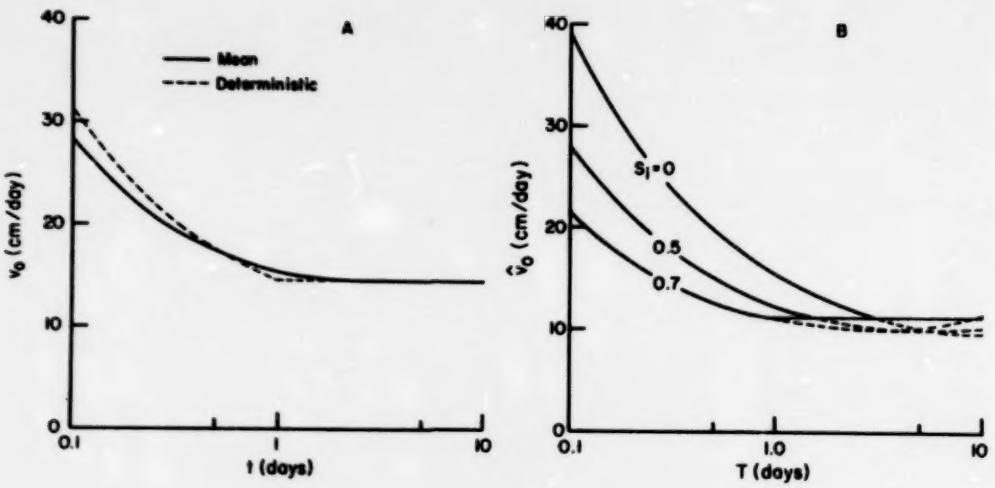

Figure 6. Intake rates for α_r = 1 (deterministic) compared to the mean values (Part A), and effect of initial condition on $\hat{v}_o$ as calculated by three terms of the semi-analytical solution (Part B).

Given is the scaled intake rate, $\hat{v}_o$, versus scaled time, T, using the algebraic results (Eq. 26). Each curve required a separate run equivalent to Table 4 in order to find corresponding A, B, and C values. Each case diverges for large times above the limiting $\hat{v}_o$ of 11.37.

The sensitivity of results to the distribution function was investigated by doubling and halving the variance of ln α. Table 5 shows the original, doubled and halved values of the variance. Also shown are the resulting A, B, and C for all three variances. The value of S_f is chosen to match the large time limiting value of Equation 15 and is smallest (0.9205) for the largest variance. This is a consequence of the domination of the overall mean by the very large values of α_r when the variance is high.

Figure 5C shows limiting ranges for v_o between the 25 and 75 percentiles for the "halved" and "doubled" variances. The mean values for all three variances were calculated separately as before and were plotted as one curve as they are nearly identical. Note for the small variance, the mean v_o is farther from the 75 percentile than the example of Figure 5B.

BEGIN LAST LINE OF TEXT
BOTTOM OF IMAGE AREA; OUTSIDE DIMENSION FOR TABLES AND ILLUSTRATIONS
3/8"

EPA-287 (Cin.)
(4-76)

BEGIN FIRST LINE OF TEXT HERE
TYPING GUIDE SHEET
CENTER OF PAGE
TOP OF IMAGE AREA
DROPPED HEAD; BEGIN SECTIONS HERE

TABLE 5. VARIANCES, S_f AND COEFFICIENTS FOR THE THREE CHOSEN DISTRIBUTIONS

Variance of ln α	$E[K^*(S_f)]$	S_f	A	B	C
.524 (Double)	6.729	.9205	18.175	2.036	.255
.262 (Original)	11.37	.9392	22.399	3.418	.584
.131 (Half)	14.77	.9481	24.845	4.430	.885

For the larger variance, the mean value is above the range for large times due to the skewness of α.

6-1/2"
9-1/8"
BEGIN LAST LINE OF TEXT
BOTTOM OF IMAGE AREA; OUTSIDE DIMENSION FOR TABLES AND ILLUSTRATIONS
3/8"

EPA-287 (Cin.)
(4-76)

BEGIN FIRST LINE OF TEXT HERE
TYPING GUIDE SHEET
CENTER OF PAGE
TOP OF IMAGE AREA
DROPPED HEAD, BEGIN SECTIONS HERE

SECTION 7

FIELD DRAINAGE--SIMPLIFIED

A simplified algebraic relation was used by Nielsen et al. (1973), to describe field drainage following ponded conditions

$$J_L = K_o/(1 + \alpha^* K_o t/L) \quad (28)$$

where J_L is the Darcian flux (cm/day), L is the depth at which the flux is considered, t is the time after drainage commences and α^* and K_o are constants describing the unsaturated conductivity. The assumptions on which Equation 28 is based are

(a) The soil is initially at a uniform moisture content, θ_o

(b) The unsaturated conductivity is

$$K = K_o \exp[\alpha^*(\theta - \theta_o)] \quad (29)$$

(c) A unit hydraulic gradient exists at all times (i.e. negligible matric gradient from the surface to depth L).

(d) Evaporation and transpiration are negligible.

Two techniques have been utilized to characterize flux with Equation 28. Warrick et al. (1977b) used Monte Carlo trials for random choices of α^* and K_o in order to find mean, variance and the frequency distribution of J_L. Rao et al. (1977) examined the same problem with a one- and two-term Taylor series expansion for the flux.

MONTE CARLO SIMULATION

The "crude" Monte Carlo technique is described by Hammersly and Handscomb (1964) and Kleijnen (1974). In our case, the K_o and α^* of Equation 28 are assumed to be log normally distributed with means and variances described in Table 6. For a given trial, a sample of n values of K_o and of α^* are chosen "randomly" from their assumed distributions. Each of the K_o and α^* values are used to calculate the flux resulting in n values of J_L. Table 6 gives results for three trials, each with n = 1000 from Warrick et al.

BEGIN LAST LINE OF TEXT
BOTTOM OF IMAGE AREA OUTSIDE DIMENSION FOR TABLES AND ILLUSTRATIONS
3/8"

EPA-287 (Cin.)
(4-76)

TABLE 6. ESTIMATES OF THE MEAN AND VARIANCE OF ln J_L AND J_L FOR THE 180-cm SOIL DEPTH USING MONTE CARLO SIMULATIONS

Trial	n	t	$E(\ln J_L)$	$Var(\ln J_L)$	$E(J_L)$	$Var(J_L)$
1	1,000	0	2.44	1.81	28.8	4,390.0
		1	0.826	0.453	2.86	1.70
		10	-1.09	0.390	0.409	0.080
2	1,000	0	2.42	1.89	28.9	4,700.0
		1	0.825	0.424	2.82	1.20
		10	-1.08	0.372	0.409	0.075
3	1,000	0	2.40	1.91	28.6	4,720.0
		1	0.821	0.447	2.84	4.55
		10	-1.08	0.371	0.409	0.075

(1977b). Even for the seemingly large samples, values from trial to trial fluctuate. When t = 0, the results are trivial since $J_L = K_o$. However, this gives an idea of the precision of the method and we compare results to $E(\ln J_L) = 2.48$ and $Var(\ln J_L) = 1.97$. The values for t = 1 and 10 days, however, are not trivial and, in fact, can only be approximated, such as by this method. Figure 7 shows the mean value (solid line) as a function of time. Also, shown by the dashed line is a "deterministic" value calculated by substituting the mean value of K_o and α^* into Equation 28. Note the solid line is consistently above the dashed line for the longer times. Also, shown by the vertical bars are the middle 50% of the values, i.e. 25% of the flux values are less than the vertical bar at each time shown and 25% are greater.

TAYLOR SERIES SOLUTION

The simplified drainage flux formula was also used by Rao et al. (1977) to approximate the mean and variance of the flux. If J_L is expanded in a Taylor series about its mean of K_o and α^*, we find

$$\mu_{J_L} = J_L(\mu_{K_o}, \mu_\alpha) + C \tag{30}$$

where C is given by

$$C = \left[\frac{\partial^2 J(\mu_{K_o}, \mu_\alpha)}{\partial K_o^2}\right]\left[\frac{\sigma_{K_o}^2}{2}\right] + \left[\frac{\partial^2 J(\mu_{K_o}, \mu_\alpha)}{\partial \alpha^2}\right]\left[\frac{\sigma_\alpha^2}{2}\right] + \left[\frac{\partial^2 J(\mu_{K_o}, \mu_\alpha)}{\partial K_o \partial \alpha}\right]\left[\frac{\rho_{K_o\alpha}\sigma_{K_o}\sigma_\alpha}{2}\right] \tag{31}$$

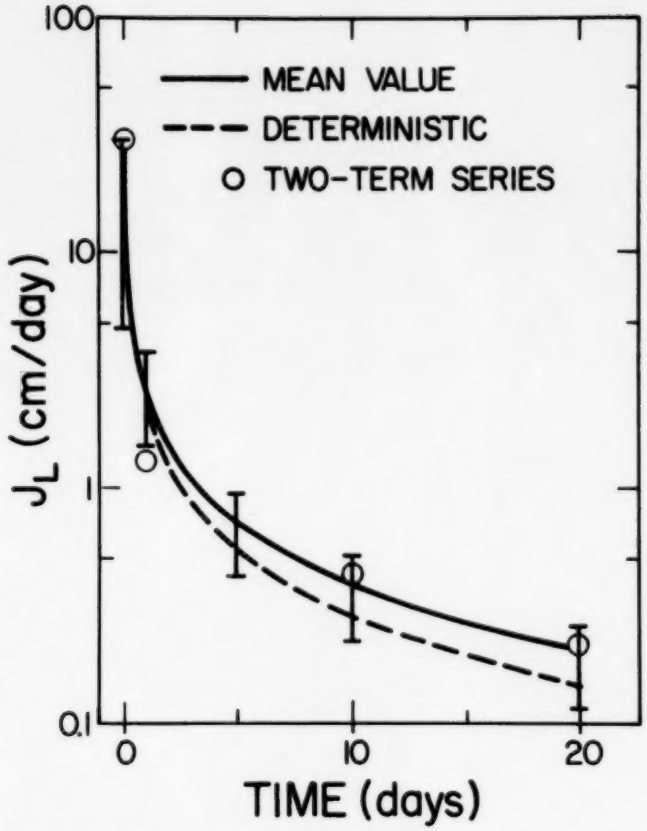

Figure 7. J_L values for t = 0 through t = 20 days for the 180-cm soil depth. The bars are ranges for the middle 50% of the values at specific times.

BEGIN FIRST LINE OF TEXT HERE
TYPING GUIDE SHEET
CENTER OF PAGE
TOP OF IMAGE AREA
DROPPED HEAD: BEGIN SECTIONS HERE

The first term is the "deterministic" value plotted in Figure 7 and is trivially the exact solution for t = 0. The two-term Taylor series of Equation 30 is also plotted on the figure. The accuracy of the Taylor series-estimates generally increases with decreasing variance of the random variables.

Variances of the flux can also be estimated by a Taylor's expansion. An expression for the variance of J_L analogous to the first term of Equation 30 is

$$\sigma_{J_L}^2 \simeq \left[\frac{\partial J_L(\mu_{K_o}, \mu_\alpha)}{\partial K_o}\right]^2 \sigma_{K_o}^2 + \left[\frac{\partial J_L(\mu_{K_o}, \mu_\alpha)}{\partial \alpha}\right]^2 \sigma_\alpha^2$$

or

$$\sigma_{J_L}^2 \simeq \frac{\sigma_{K_o}^2 + (t/L)^2 \mu_{K_o}^4 \sigma_\alpha^2}{[1 + (t/L)\mu_{K_o}\mu_\alpha]^4} \qquad (32)$$

6-1/2"

DRAINAGE FOLLOWING UNIFORM SPRINKLING

If we have a constant flux over the entire area, and then stop the irrigation at time zero, a simplified form for the flux equivalent to the ponded water case is (Warrick, 1977)

$$J_L = I_o/(1 + \alpha^* I_o t/L) \qquad (33)$$

where I_o is the initial rate. Since we assume I_o constant, Equation 33 is simpler than Equation 28 in that α^* is the only uncertain parameter.

The mean value of J_L was determined by a Monte Carlo simulation, normalized by I_o and plotted as a function of time in Figure 8, with I_o = 2.6 cm/day. At t = 0, all of the J_L values are simply the constant I_o. As time progresses, we see effects of the variability. The mean values are again consistently above the deterministic value found by substituting the mean α^* value into Equation 33. Also shown as the shaded region is a band of values corresponding to the middle 50% of the flux values as before. The middle 50% of values can be found analytically in this case since the high 25% of J_L values correspond to the low 25% of the α^* values and vice versa.

BEGIN LAST LINE OF TEXT
BOTTOM OF IMAGE AREA; OUTSIDE DIMENSION FOR TABLES AND ILLUSTRATIONS
3/8"

EPA-287 (Cin.) (4-76)

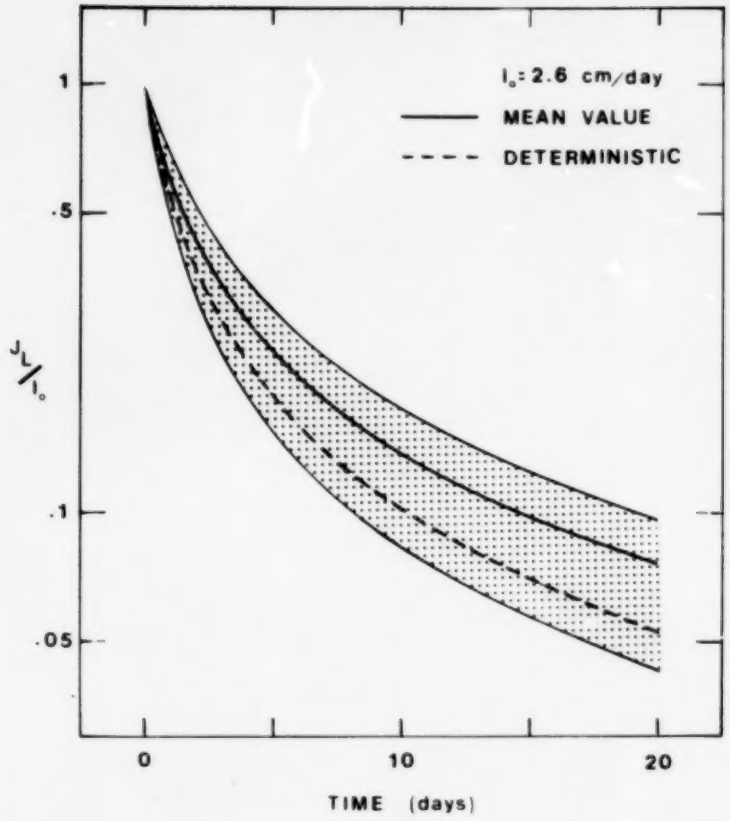

Figure 8. Flux values as a function of time for drainage following uniform sprinkling. Shaded area is for the middle 50% of values.

BEGIN FIRST LINE OF TEXT HERE
TYPING GUIDE SHEET
CENTER OF PAGE
TOP OF IMAGE AREA
DROPPED HEAD BEGIN SECTIONS HERE
6-1/2"
9-1/8"

SECTION 8

FIELD DRAINAGE--NON-LINEAR ANALYSIS

For general conditions, the non-linear moisture flow equation (Eq. 7) can be solved only by numerical techniques. Unfortunately, no semi-analytical solution exists for drainage such as was so convenient in the case of infiltration. However, we can take advantage of the scaled form of Equation 10 in order to minimize calculations. Our basic approach is to solve the scaled moisture flow equation one time using a finite difference scheme. Site specific results are found by interpolating from the basic solution array.

We assume that the profile is initially at a constant degree of saturation $S = S_i$ with drainage commencing at time $t = 0$ without surface loss. The average value of S from 0 to $x = L$ is given by

$$S_{avg} = (1/\alpha_r L)\int_0^{\alpha_r L} S dX \qquad (34)$$

Thus, the average value of S at any time T is a function of the scaled depth $\alpha_r L$. Similarly, the flux given by

$$v = -D(\partial\theta/\partial x) + K$$

can be expressed as

$$v_r = \alpha_r^2 \hat{v} \qquad (35)$$

where the scaled flux $\hat{v}$ is

$$\hat{v} = -\hat{D}(\partial S/\partial X) + \hat{K} \qquad (36)$$

Calculations were performed using the Panoche data (Warrick et al., 1977a) and Equation 11. The initial value $S = S_i$ was also chosen to match the average ponded data, resulting in $S_i = 0.939$ for the drainage example.

The finite difference algorithm used is after Rubin and Steinhardt (1963) and the FORTRAN program is given as the Appendix. The moisture flow equation is approximated by an implicit form

$$-A_j S_{j+1}^{n+1} + B_j S_j^{n+1} - C_j S_{j-1}^{n+1} = H_j \qquad (37)$$

where

BEGIN LAST LINE OF TEXT
3/8"
BOTTOM OF IMAGE AREA OUTSIDE DIMENSION FOR TABLES AND ILLUSTRATIONS

PAGE NUMBER
EPA-287 (Cin.) (4-76)

BEGIN FIRST LINE OF TEXT HERE
TYPING GUIDE SHEET
CENTER OF PAGE
TOP OF IMAGE AREA
DROPPED HEAD. BEGIN SECTIONS HERE

$$A_j = (\Delta T/\Delta X^2)(D^{n+\frac{1}{2}}_{j+\frac{1}{2}}) \tag{38}$$

$$C_j = (\Delta T/\Delta X^2)\, D^{n+\frac{1}{2}}_{j-\frac{1}{2}} \tag{39}$$

$$B_j = 2 + A_j + C_j \tag{40}$$

$$H_j = A_j S^n_{j+1} + (2 - A_j - C_j)S^n_j + C_j S^n_{j-1} - 2(\Delta T/\Delta X)\{K^{n+\frac{1}{2}}_{j+\frac{1}{2}} - K^{n+\frac{1}{2}}_{j-\frac{1}{2}}\} \tag{41}$$

with $K^{n+\frac{1}{2}}_{j\pm\frac{1}{2}}$ and $D^{n+\frac{1}{2}}_{j\pm\frac{1}{2}}$ evaluated as the conductivity or diffusivity functions corresponding to estimated water contents.

$$S^{n+\frac{1}{2}}_{j\pm\frac{1}{2}}\Big|_{est} = (3/4)(S^n_{j+\frac{1}{2}\pm\frac{1}{2}} + S^n_{j-\frac{1}{2}\pm\frac{1}{2}}) - (1/4)(S^{n-1}_{j+\frac{1}{2}\pm\frac{1}{2}} + S^{n-1}_{j-\frac{1}{2}\pm\frac{1}{2}}) \tag{42}$$

6-1/2"

Initial and boundary conditions are

$$S(X,0) = S_i \tag{43}$$

9-1/8"

$$-D(\partial S/\partial X) + K = R(t), \quad X = 0 \tag{44}$$

$$\partial S/\partial X = 0, \quad X = X_o \tag{45}$$

with S_i the constant initial moisture value, R(t) is the rate of application and X_o is the lower depth at which the hydraulic gradient is taken to be unity (i.e. moisture content gradient taken to be zero). For the drainage case, R(t) of Equation 44 is set equal to zero.

The finite difference form of Equation 44 is

$$-D^{n+\frac{1}{2}}_{\frac{1}{2}}(\partial S/\partial X)^{n+\frac{1}{2}}_{\frac{1}{2}} + K^{n+\frac{1}{2}}_{\frac{1}{2}} = R \tag{46}$$

with the grid set in such a way as to make X = 0 coincide with the line $j = \frac{1}{2}$.

For the computations, $\hat{K}$ and $\hat{h}$ from Equations 5 and 6 were used. A step size $\Delta X = 8$ was chosen for the depth with the time steps ΔT ranging between 0.00036 and 0.02. Results were stored in a two-dimensional array similar to that shown in Table 7 for each scaled depth and time, S_{avg} and $\hat{v}$. (Values were not rounded off further because differences are significant during interpolation.) The value of $\hat{V}$ can be found based on a rate of change in mass, i.e.

$$\hat{v} = X\,\theta_s(S_{avg}|_T - S_{avg}|_{T-\Delta T})\Delta T \tag{47}$$

BEGIN LAST LINE OF TEXT
BOTTOM OF IMAGE AREA, OUTSIDE DIMENSION FOR TABLES AND ILLUSTRATIONS
3/8"

EPA-287 (Cin.)
(4-76)

TABLE 7. VALUES OF S_{avg} AND SCALED FLUX $\hat{v}$ AS FUNCTIONS OF X AND T FOR DRAINAGE (The numbers have deliberately not been rounded, see text)

$X = \alpha_r X$		$T = (\alpha_r^3/\theta_s)t$ 0.0	0.25	0.5	1.0	2.0	5.0
4.0	S_{avg}	.93924	.88248	.86408	.84250	.81782	.78055
	$\hat{v}$	11.36742	.67569	.40579	.23706	.13584	.06417
12.0	S_{avg}	.93924	.89196	.87397	.85197	.82729	.79010
	$\hat{v}$	11.36742	1.14525	.68081	.39262	.22188	.10302
20.0	S_{avg}	.93924	.89940	.88119	.85971	.83515	.79815
	$\hat{v}$	11.36742	1.92230	1.14565	.66081	.37314	.17302
28.0	S_{avg}	.93924	.90542	.88750	.86620	.84181	.80508
	$\hat{v}$	11.36742	2.68056	1.60426	.92630	.52298	.24236
36.0	S_{avg}	.93924	.91042	.89235	.87177	.84758	.81113
	$\hat{v}$	11.36742	3.41723	2.05620	1.18905	.67141	.31105
44.0	S_{avg}	.93924	.91464	.89746	.87662	.85263	.81649
	$\hat{v}$	11.36742	4.12977	2.40109	1.44908	.81846	.37909

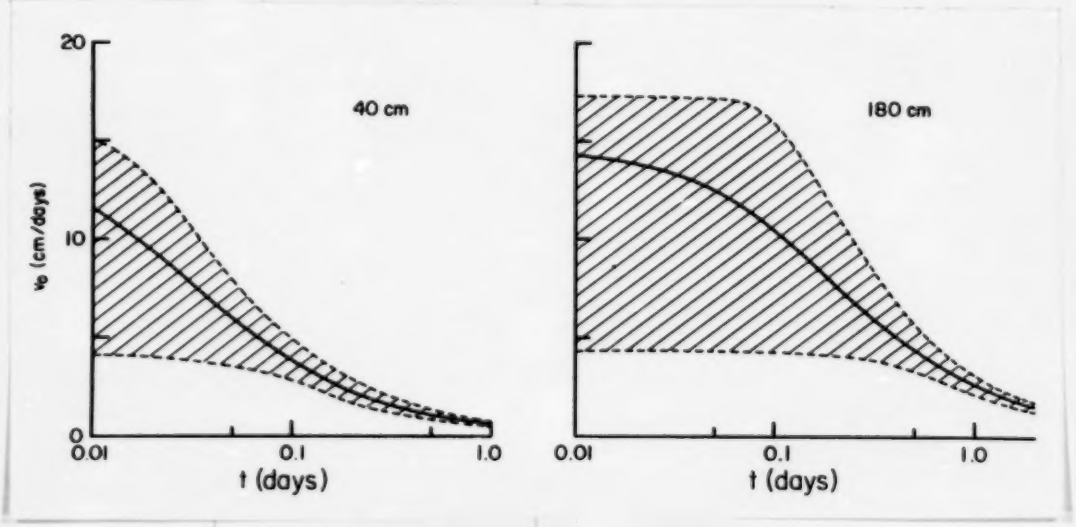

Figure 9. Mean drainage velocities at the 40-cm (A) and 180-cm (B) depths (solid lines). The 25 and 75 percentiles are shown by dashed lines.

BEGIN FIRST LINE OF TEXT HERE
TYPING GUIDE SHEET
CENTER OF PAGE
TOP OF IMAGE AREA
DROPPED HEAD. BEGIN SECTIONS HERE

For any real depth and time within the range of the table, S_{avg} and $\hat{v}$ can be estimated by interpolation. For specified α_r, we calculate the corresponding scaled depth X and scaled time T. We then find the closest X and T values in the table and interpolate.

The mean flux density v_o for the 40- and 180-cm depths are shown as Figure 9, following a Monte Carlo simulation. First, an array similar to Table 7 was set up for 41 depths (to X = 324) and 24 times (to T = 40) using the finite difference solution. Once the table was set up and stored on magnetic tape, random values of α_r were chosen and dimensionless X and T values were found. The corresponding average S and v were found by two-way linear interpolation. The resulting average for 1000 such α_r is plotted showing the decrease in average flux with time. Also shown as the shaded area is the middle 50% of flux values. Twenty-five percent of the values at any time are above the upper limit and 25 percent are below the lower limit.

CYCLICAL WATER APPLICATION

For cyclic water applications, we use a simplification of Equation 11. namely a linearized form after Warrick (1975)

$$\partial S/\partial T = D^*(\partial^2 S/\partial X^2) - k^*(\partial S/\partial X) \qquad (48)$$

where D* and k* are linearized constants with D* (units L^2/T) equivalent to $\hat{D}$ and k* given approximately by $(1/\theta_s)(dK/dS)$. Although the non-linear form would be more general, the solution of Equation 48 is much easier and allows us to set up the procedure with less effort. In addition, the cyclic case is somewhat adequately described using the linearized form.

Our boundary conditions are in terms of the specific flux (units L/T)

$$\begin{aligned} f = f_o, \quad & x = 0, \ 0 < t < t_1 \\ & \quad\ t_2 < t < t_3 \\ & \quad\ t_4 < t < t_5 \\ & \quad\ \vdots \\ f = 0, \quad & x = 0, \ t_1 < t < t_2 \\ & \quad\ t_3 < t < t_4 \\ & \quad\ \vdots \end{aligned} \qquad (49)$$

Thus, water is added to the surface in pulses. The pulses are assumed to be equally spaced, such that

BEGIN LAST LINE OF TEXT HERE
BOTTOM OF IMAGE AREA, OUTSIDE DIMENSION FOR TABLES AND ILLUSTRATIONS
3/8"

EPA-287 (Cin.) (4-76)

BEGIN FIRST LINE OF TEXT HERE
TYPING GUIDE SHEET
CENTER OF PAGE
TOP OF IMAGE AREA
DROPPED HEAD, BEGIN SECTIONS HERE

$$t_{2n+1} - t_{2n} = \Delta t_{wet} \tag{50}$$

$$t_{2n} - t_{2n-1} = \Delta t_{dry},\ n = 1, 2, \ldots$$

Thus Δt_{wet} is the period that water is added for each cycle, Δt_{dry} is the time for which no water is added. The flux at infinity, f_∞, is the average rate of water added, thus

$$f_\infty = f_o \Delta t_{wet}/(\Delta t_{wet} + \Delta t_{dry}) \tag{51}$$

For larger times, the effect of the initial condition becomes less and less important. Thus, without loss of generality, we take the initial condition to be zero.

The solution of Equation 48 with the specified boundary conditions is by Warrick (1975, especially Equations 18 and 20).

$$S(X,T) = \sum_{i=0}^{N} (B_i - B_{i-1})\theta_U(k^*X/D^*, k^{*2}T/D^* - k^{*2}T_i/D^*) \quad , T > T_N \tag{52}$$

$$(B_{-1} = 0, \quad T_o = 0)$$

$$B_{2n} = (\hat{f}_o - \hat{f}_\infty)/k^*S_\infty$$

$$B_{2n+1} = -\hat{f}_\infty/(k^*S_\infty) \qquad n = 0, 1, 2, \ldots \tag{53}$$

$$T_{2n} = n(\alpha^3/\theta_s)(\Delta t_{wet} + \Delta t_{dry})$$

$$T_{2n+1} = T_{2n} + (\alpha^3/\theta_s)\Delta t_{wet} \qquad n = 0, 1, 2, \ldots \tag{54}$$

$$\theta_U(u,v) = -[\exp(u)/2](u + v + 1)\operatorname{erfc}(u/2\sqrt{v} + \sqrt{v}/2)$$

$$+ \sqrt{v/\pi}\, \exp[-(u/2\sqrt{v} - \sqrt{v}/2)^2]$$

$$+ (1/2)\operatorname{erfc}(u/2\sqrt{v} - \sqrt{v}/2) \tag{55}$$

and S_∞ is the limiting value of S for large depths and corresponds to f_∞. The reduced fluxes $\hat{f}_o$ and $\hat{f}_\infty$ are given by f_o/α^2 and f_∞/α_r^2, respectively.

For calculations, we use data from Warrick et al. (1977a). The log α is assumed to be normally distributed with mean of -0.136 and standard deviation 0.512. A one-day cycle is chosen with water added for two hours at a constant rate of 12 cm/day followed by 22 hours of drainage. Thus, the total input is one cm for each day and the average flux is f_∞ = 1 cm/day also. Values of k* and D* were 99 cm/day and 2500 cm^2/day, respectively, with θ_s = 0.45 cm^3/cm^3.

Moisture profiles are shown after one hour into the cycle in Figure 10a. The 11th cycle was used in order to avoid effects of the initial condition. The middle solid line is for the "deterministic" value found by taking the mean value of α = 0.995. The shaded region from left to right is for the 75 to 25 percentile. In order to interpret the results, it is important to

BEGIN LAST LINE OF TEXT
BOTTOM OF IMAGE AREA; OUTSIDE DIMENSION FOR TABLES AND ILLUSTRATIONS
3/8"

EPA-287 (Cin.)
(4-76)

BEGIN FIRST LINE OF TEXT HERE
TYPING GUIDE SHEET
CENTER OF PAGE
TOP OF IMAGE AREA
DROPPED HEAD; BEGIN SECTIONS HERE

remember that the flux during the wet part of the cycle is a constant and independent of the value of α. The profile which has the highest value of α tends to take in the water easier and consequently does not wet up as much. The value of $S = S_\infty$ at large depths is found by

$$f_\infty = \alpha^2 \hat{K}(S_\infty) \tag{56}$$

with the function $\hat{K}$ by Equation 6. If α is large, then S is small and vice versa. Thus, the values for the 75, deterministic and 25 percentile are $\theta = 0.367$, 0.377 and 0.397, respectively, and are shown by the lower part of each graph.

Figure 10b is at the end of the wetting part of the cycle. Note all of the profiles have wetted up somewhat over the values of Figure 10a. Also shown are values one-half of the way through the dry part of the cycle (Figure 10c) and at the end of the dry cycle (Figure 10d). (The sketch in the lower center shows where each is located within the time cycle.) The profiles for the drying part of the cycle are somewhat vertical and show nearly a unit hydraulic gradient. The values of S_∞ are the same as for the wetting parts of the cycle.

In Figure 11 the cyclic values of θ are plotted as a function of time for the surface and the 40-cm depths. For both cases, the solid line shows the deterministic value and the shaded region shows the range between the 25 and 75 percentile values. The 25 percentile shows the largest fluctuation with deterministic intermediate and the 75 percentile shows the smallest or least fluctuation. Also, note that the 40-cm depth shows much smaller fluctuations, tends to undergo a more gradual transition and lags slightly behind the surface curve.

BEGIN LAST LINE OF TEXT
BOTTOM OF IMAGE AREA; OUTSIDE DIMENSION FOR TABLES AND ILLUSTRATIONS
3/8"

EPA-287 (Cin.)
(4-76)

BEGIN FIRST LINE OF TEXT HERE
TYPING GUIDE SHEET
CENTER OF PAGE
TOP OF IMAGE AREA
DROPPED HEAD; BEGIN SECTIONS HERE

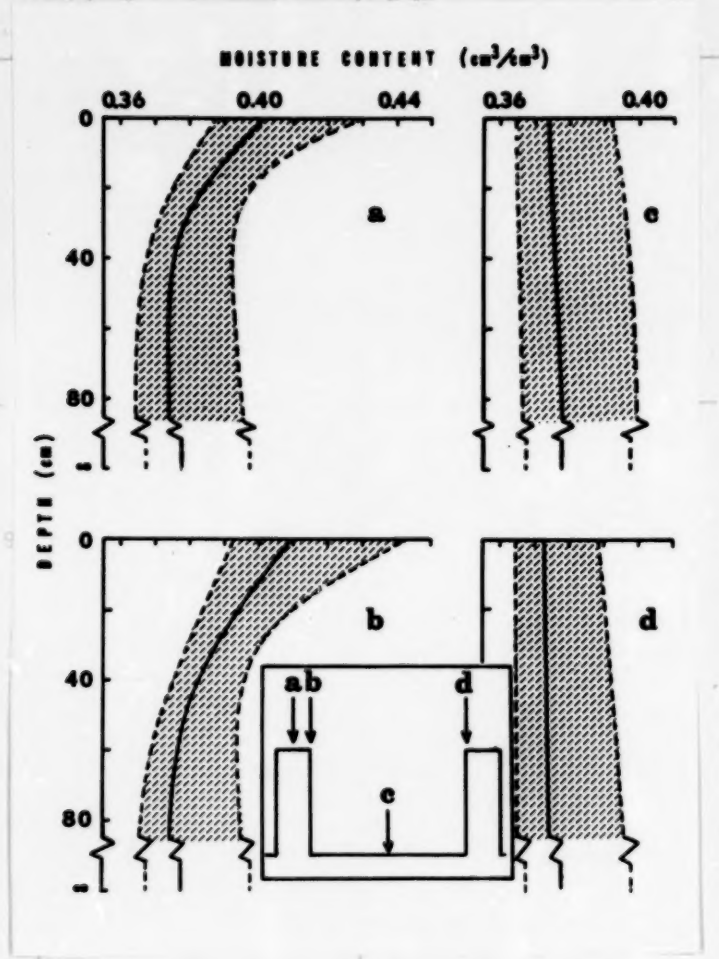

Figure 10. Moisture profiles at 1, 2, 13, and 24 hours (a, b, c, and d, respectively) into cycle for high frequency irrigation. In each sketch, the three curves from left to right are the 75 percentile, the mean and the 25 percentile values of the scaling coefficient.

BEGIN LAST LINE OF TEXT
BOTTOM OF IMAGE AREA OUTSIDE DIMENSION FOR TABLES AND ILLUSTRATIONS
3/8"

PAGE NUMBER
EPA-287 (Cin.) (4-76)

BEGIN FIRST LINE OF TEXT HERE
TYPING GUIDE SHEET
CENTER OF PAGE
TOP OF IMAGE AREA
DROPPED HEAD; BEGIN SECTIONS HERE

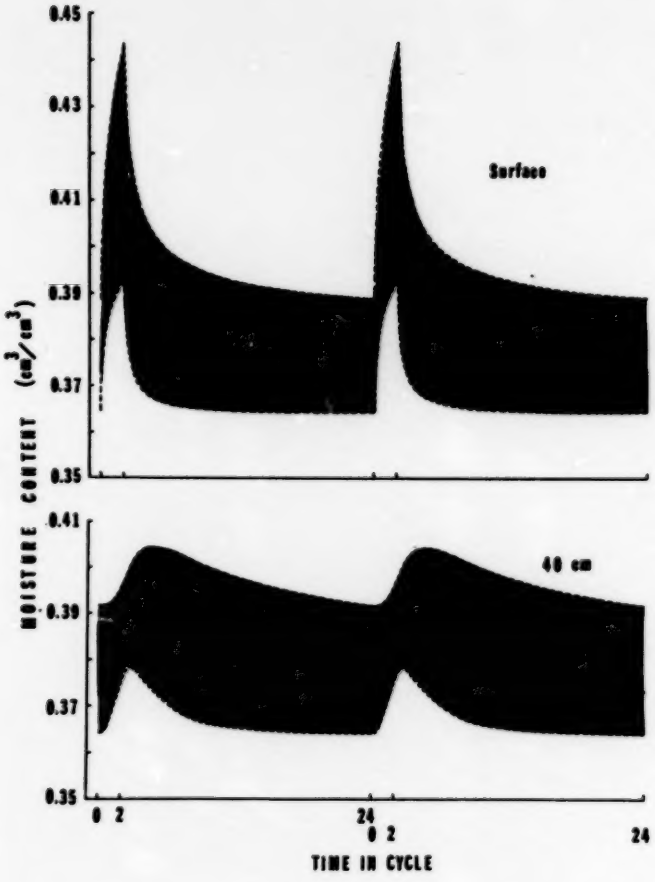

Figure 11. Values of moisture content during the 24-hour cycle at the surface and the 40-cm depth. The lower, middle and upper curves in each case are for the 75 percentile, the mean and the 25 percentile values of the scaling coefficient, respectively.

BEGIN LAST LINE OF TEXT
BOTTOM OF IMAGE AREA; OUTSIDE DIMENSION FOR TABLES AND ILLUSTRATIONS
3/8"

EPA-287 (Cin.)
(4-76)

BEGIN FIRST LINE OF TEXT HERE
TYPING GUIDE SHEET
CENTER OF PAGE
TOP OF IMAGE AREA
DROPPED HEAD; BEGIN SECTIONS HERE

SECTION 9

SOLUTE MOVEMENT

Movement of salts is strongly dependent on soil water fluxes. Soluble ions such as chloride, nitrate, and sodium move readily with water. Even strongly adsorbed ions, organic molecules or reactive materials are transported with the water. Thus, the variability of soil water velocity is a strong factor on such processes as leaching and solute emissions from irrigated fields.

In addition to variations in the soil water movement, there are also variations of solutes within the profile, both inherently and by past management practices. Furthermore, the apparent diffusion coefficients, reaction coefficients and perhaps other parameters also may be expected to have a variable pattern with space.

In this study, we simulate salts moving with the water. The apparent diffusion coefficient and soil water velocity are assumed to vary with surface position in a field, but not with depth. At any particular location within the field, only a simple flow system is considered having (1) steady vertical velocity which is independent of depth, (2) negligible solute-soil interaction, and (3) no horizontal movement. The solute is added with the surface water in a pulse, that is by injecting or mixing with the water over a short finite time period.

THEORY

The appropriate differential equation describing non-interacting solute flow is

$$\partial c/\partial t = D(\partial^2 c/\partial x^2) - v(\partial c/\partial x) \qquad (57)$$

with c the soil solute concentration, D the apparent diffusion coefficient (units L^2/T), v the pore water velocity (units L/T and equal to the Darcian velocity divided by water-filled porosity), x the vertical depth of the soil and t time. The boundary conditions for a "pulse" of solute introduced at the surface is

$$\begin{aligned} c(0,t) &= 0, & t < 0 \\ &= c_o, & 0 < t < t_o \\ &= 0, & t > t_o \end{aligned} \qquad (58)$$

BEGIN LAST LINE OF TEXT
BOTTOM OF IMAGE AREA; OUTSIDE DIMENSION FOR TABLES AND ILLUSTRATIONS
3/8"

EPA-287 (Cin.)
(4-76)

BEGIN FIRST LINE OF TEXT HERE
TYPING GUIDE SHEET
CENTER OF PAGE
TOP OF IMAGE AREA
DROPPED HEAD; BEGIN SECTIONS HERE

The initial condition is taken to be

$$c(x,0) = 0 \tag{59}$$

The solution of Equation 57 subject to Equation 59 is by Warrick et al. (1971) and elsewhere

$$c(x,t) = (c_o/2)\{\text{erfc}[\frac{x-vt}{2\sqrt{Dt}}] + \exp(vx/D)\text{erfc}[\frac{x+vt}{2\sqrt{Dt}}]\},$$

$$0 < t < t_o \tag{60}$$

$$c(x,t) = (c_o/2)\{\text{erfc}[\frac{x-vt}{2\sqrt{Dt}}] + \exp(vx/D)\text{erfc}[\frac{x+vt}{2\sqrt{Dt}}] - \text{erfc}[\frac{x-v(t-t_o)}{2\sqrt{D(t-t_o)}}]$$

$$- \exp(vx/D)\text{erfc}[\frac{x+v(t-t_o)}{2\sqrt{D(t-t_o)}}]\}, \qquad t > t_o \tag{61}$$

They also present an approximate solution for the maximum concentration of the pulse as it travels downward through the profile.

$$c = c_o \text{ erf}(a/2\sqrt{Dt}) \tag{62}$$

with "a" equal to one-half of the initial width of the solute band in the soil

$$a = vt_o/2 \tag{63}$$

The location of the maximum concentration is at approximately

$$x_{max} = vt - a \tag{64}$$

The effect of varying the apparent diffusion coefficient, D, while holding v constant, is shown schematically in Figure 12A and 12B. (Also see Biggar and Nielsen, 1976, Figure 9.) For "small" D, the solute proceeds through the soil profile with minimum dispersion, i.e. with little spreading and with the high maximum concentration maintained. For a high value of D the solute is spread out over a larger depth and the maximum concentration is less. In both cases the area under the curves is the same. (We assume no solute is gained or lost to the soil solids and the water-filled porosity is constant.)

For v varying but D constant, we present Figures 12C and 12D. The value of v merely reflects the translation velocity, so for any given time the smaller v results in the solute pulse moving a lesser distance and the larger v gives a deeper displacement. If D is the same in both cases, the shape of the solute profile remains the same.

In real situations, neither D nor v will be constant. In fact, they will be related although not necessarily in a simple fashion. The problem we address is evaluating the maximum concentration as a consequence of D and v

BEGIN LAST LINE OF TEXT HERE
BOTTOM OF IMAGE AREA; OUTSIDE DIMENSION FOR TABLES AND ILLUSTRATIONS
3/8"

EPA-287 (Cin.) (4-76)

TYPING GUIDE SHEET
BEGIN FIRST LINE OF TEXT HERE
CENTER OF PAGE
TOP OF IMAGE AREA
DROPPED HEAD: BEGIN SECTIONS HERE

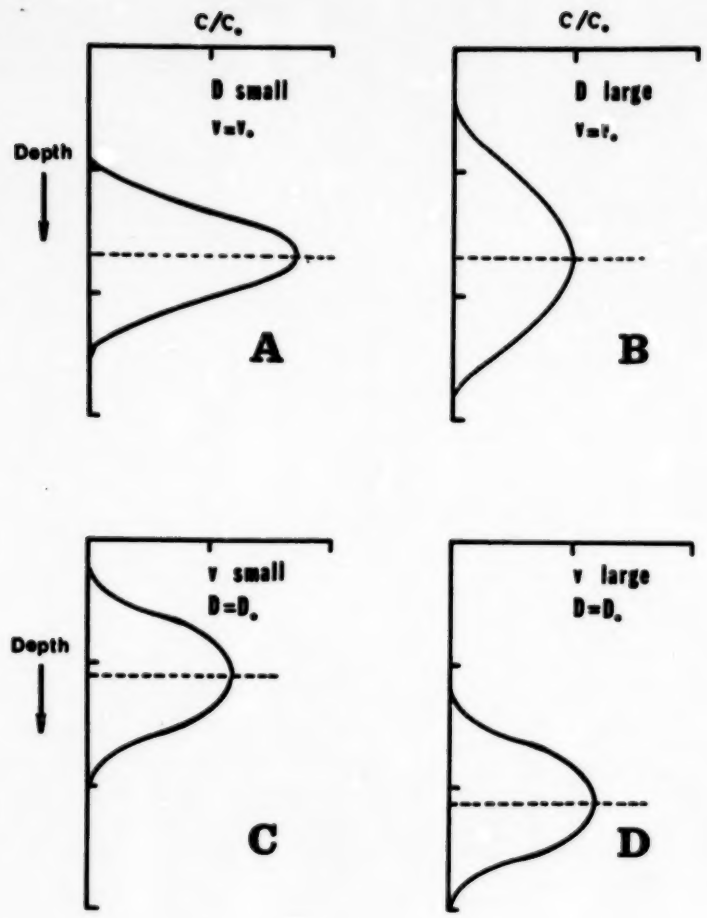

Figure 12. Effect of changing apparent diffusion coefficient D (Parts A and B) and the velocity v (Parts C and D).

BEGIN LAST LINE OF TEXT HERE
BOTTOM OF IMAGE AREA; OUTSIDE DIMENSION FOR TABLES AND ILLUSTRATIONS
3/8"

EPA-287 (Cin.)
(4-76)

varying in different ways. Also, we are interested in the statistical distribution of the results.

FIELD DATA

The input data for D and v were chosen after Biggar and Nielsen (1976) (see Table 1). As stated, they conducted detailed field experiments on Panoche loam, an alluvial soil in the San Joaquin Valley of California. Twenty plots, each 6 by 6 m, were flooded. A pulse of 7.6 cm of 0.2 normal $CaCl_2$ solution was added with salt concentration and water contents monitored at 30, 60, 90, 120, 150, and 180 cm. Roughly speaking, they found D (cm^2/day) to be log normally distributed with log D having a mean of 4.42 and a standard deviation of 1.74. Similarly, the pore water velocity, v, (cm/day) was found to be approximately log normal with mean and standard deviation of log v of 3.01 and 1.25. The value of D tended to increase with increasing v approximately as

$$D = 0.6 + 2.93\ v^{1.11} \qquad (65)$$

with the fitting correlation coefficient r = 0.80.

NUMERICAL EXAMPLES

Calculations were performed for the eight choices of convective velocity, v, and apparent diffusion coefficient, D, given in Table 8. For the first six combinations (Cases I-VI), Equations 60 and 61 were used and for the last two cases (I' and II') the simplified Equation 62 was employed. In all the calculations, the water-filled porosity was 0.4 cm^3/cm^3. For the "pulse" cases 7.5 cm^3/cm^2 of water was added at the soil surface.

The simplest solution is to use the mean values v = 44 cm/day and D = 378 cm^2/day (Case I). Results are given in Figure 13 for a "step input", i.e. for a salt solution added continuously at the soil surface after time zero. The profile given in the figure is after five days and shows the well known sigmoid pattern. For Case II, v is constant as before, but D is assumed to be log normally distributed and must be evaluated as a Monte Carlo simulation. Briefly, this procedure is to

(1) Draw a random value from a population which is normally distributed with variance of one.

(2) Calculate the corresponding random D by setting the random value equal to (ln D - 4.42)/1.74.

(3) Calculate a random c/c_0 from the appropriate equation with D from above and v = 44 for each t and x value of interest.

(4) Repeat (1) through (3), 2000 times and find the mean of these results for each space and time combination.

TABLE 8. CHOICES OF APPARENT DIFFUSION COEFFICIENT, D, AND CONVECTIVE VELOCITY, v, FOR MONTE CARLO SIMULATIONS OF MEAN SOLUTE DISTRIBUTION AND FLUXES

Case	Convective Velocity v	Apparent Diffusion Coefficient D
I	Constant (44 cm/day)	Constant (378 cm^2/day)
II	"	Variable $\ln D \sim N(4.42, 1.74^2)$
III	Variable $\ln v \sim N(3.01, 1.25^2)$	Zero
IV	"	Constant (378 cm^2/day)
V	"	Variable (Independent of v)
VI	"	$0.6 + 2.93\ v^{1.11}$
I' and II'	(Same as Cases I and II, but with simplified Equation 62.)	

The calculations were performed on the high-speed digital computer (Control Data Corporation "CYBER 175") available at the University of Arizona. The normally distributed random values are as from Maisel and Gnugnoli (1972, especially p. 153).

The Case II results are plotted alongside those of Case I in Figure 13 for the step input. The curve is also sigmoid with the center practically at the same depth. The curve is more abrupt than before. The interpretation of the curve is as follows:

(1) The center of the curve will be at the same depth for constant v whether for Case I, Case II or the simpler case with D = 0. The depth is given almost exactly in each case by vt = (44 cm/day)(5 days) = 220 cm.

(2) The distribution of D is highly skewed. Thus, the median value of D is considerably less than the mean. As many values of D are much smaller than the mean, the average of the c/c_o at any depth should be closer to a "piston" displacement which is precisely what the results show. If we chose a smaller D, it would give results closer to Case II.

The results for a 7.5-cm pulse are given in Figure 14. The maximum values for Cases I and II are at about the same depth. However, the large mean of D again shows more spreading (Case I) whereas the Case II is characterized by less dispersion and consequently a larger maximum value.

Flux distributions for Cases I and II are shown for step and pulse inputs for the 60 and 180-cm depths in Figures 15-18. The relationships for Cases I and II thorughout these four comparisons are about the same but with

BEGIN FIRST LINE OF TEXT HERE
TYPING GUIDE SHEET
CENTER OF PAGE
TOP OF IMAGE AREA
DROPPED HEAD; BEGIN SECTIONS HERE

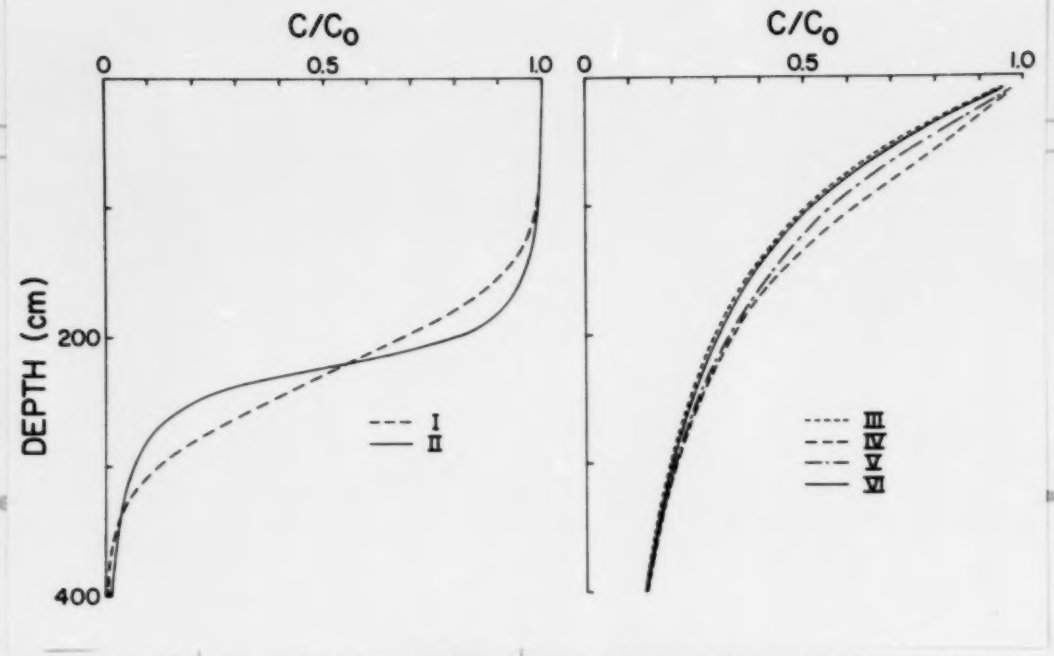

Figure 13. Average relative solute concentration with depth for a step input after five days

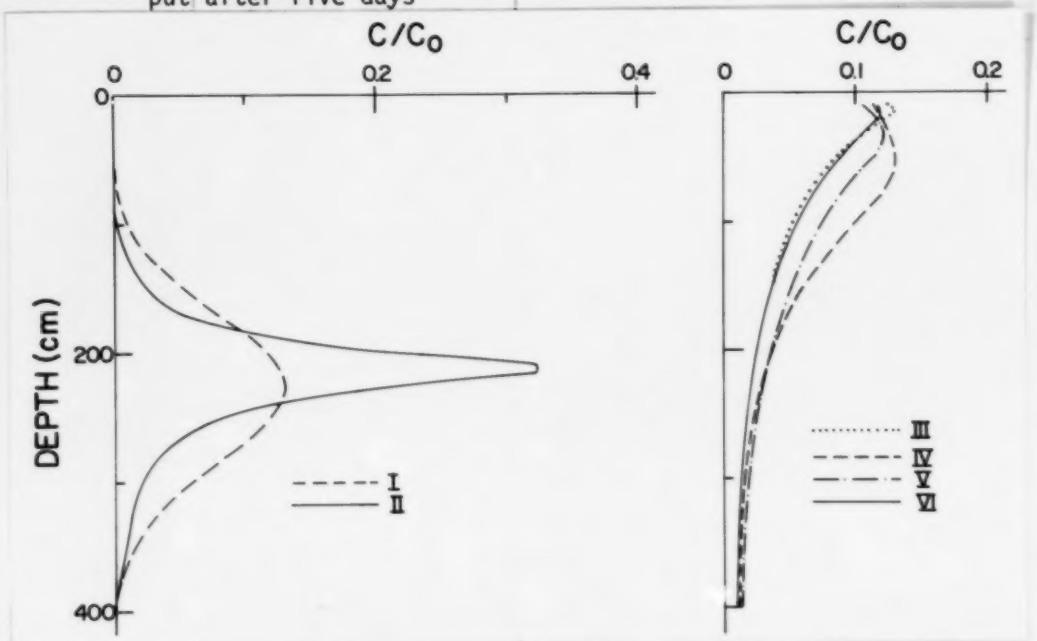

Figure 14. Average relative solute concentration with depth for a 7.5-cm pulse of salt water after five days.

BEGIN LAST LINE OF TEXT
BOTTOM OF IMAGE AREA; OUTSIDE DIMENSION FOR TABLES AND ILLUSTRATIONS
3/8"

PAGE NUMBER
EPA-287 (Cin.)
(4-76)

BEGIN FIRST LINE OF TEXT HERE
TYPING GUIDE SHEET
CENTER OF PAGE
TOP OF IMAGE AREA
DROPPED HEAD; BEGIN SECTIONS HERE

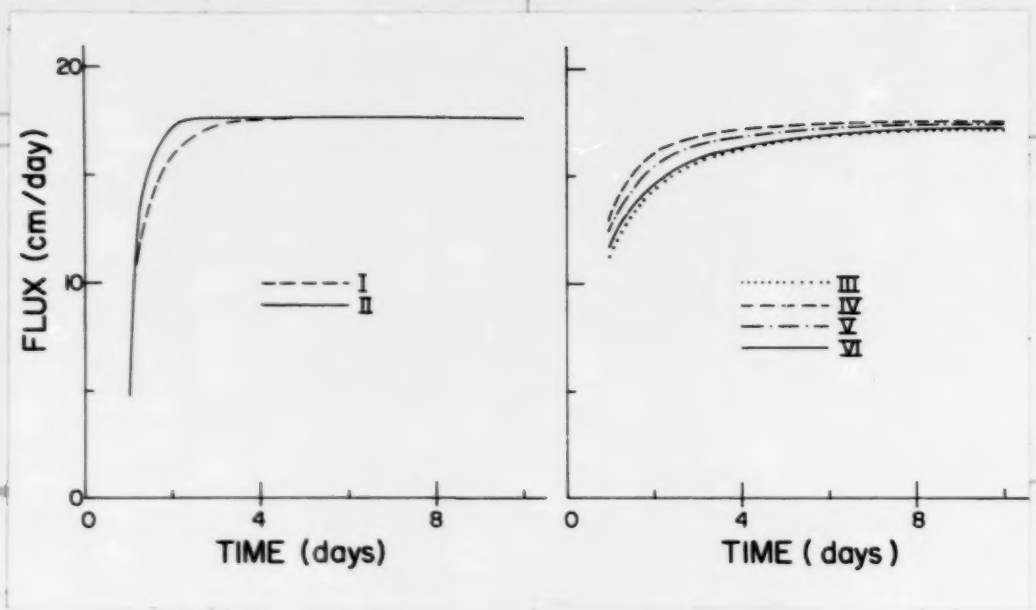

Figure 15. Average solute flux at 60-cm depth for a step input.

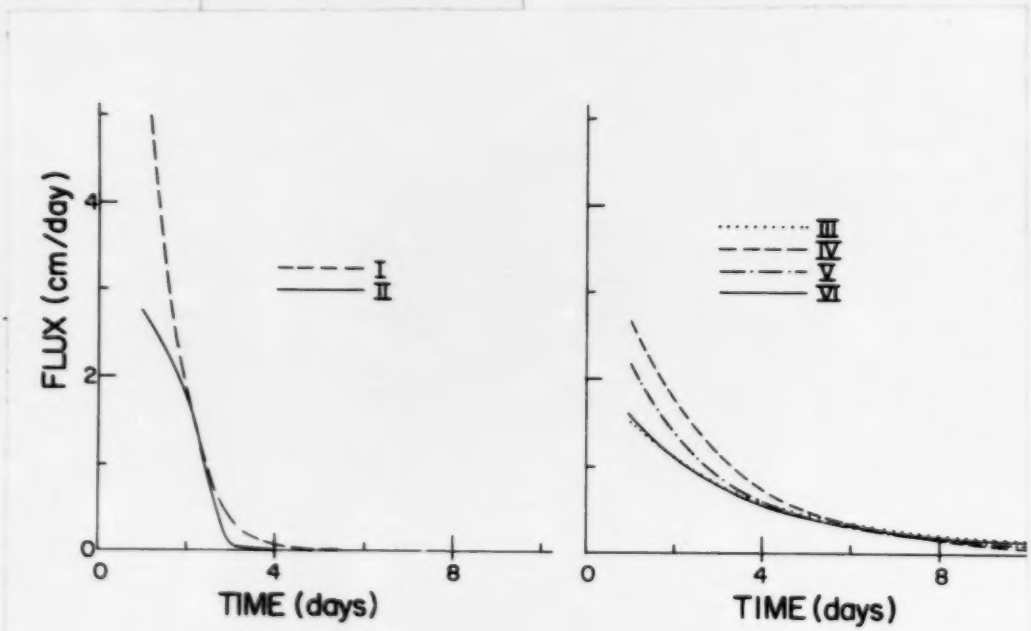

Figure 16. Average solute flux at 60-cm depth for a pulse input.

BEGIN LAST LINE OF TEXT HERE
BOTTOM OF IMAGE AREA; OUTSIDE DIMENSION FOR TABLES AND ILLUSTRATIONS
3/8"

EPA-287 (Cin.)
(4-76)

BEGIN FIRST LINE OF TEXT HERE
TYPING GUIDE SHEET
CENTER OF PAGE
TOP OF IMAGE AREA
DROPPED HEAD; BEGIN SECTIONS HERE

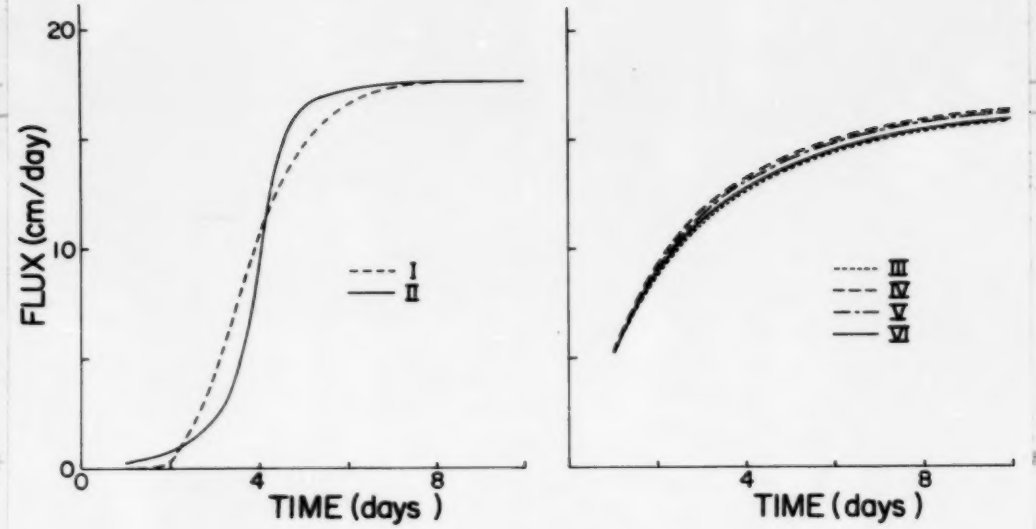

Figure 17. Average solute flux at 180-cm depth for a step input.

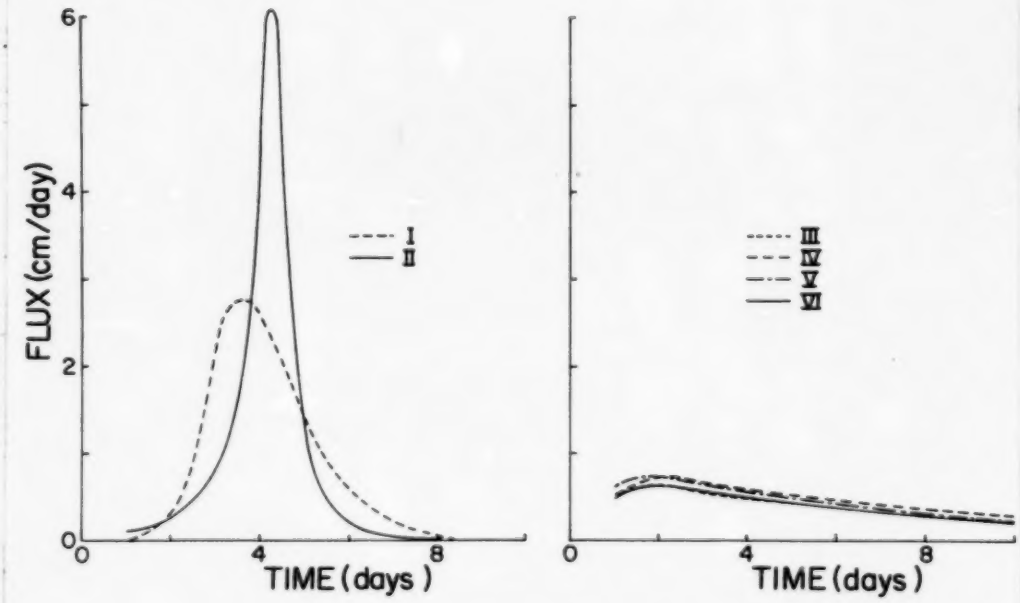

Figure 18. Average solute flux at 180-cm depth for a pulse input.

BEGIN LAST LINE OF TEXT
BOTTOM OF IMAGE AREA; OUTSIDE DIMENSION FOR TABLES AND ILLUSTRATIONS
3/8"
PAGE NUMBER
EPA-287 (Cin.)
(4-76)

BEGIN FIRST LINE OF TEXT HERE
TYPING GUIDE SHEET
CENTER OF PAGE
TOP OF IMAGE AREA
DROPPED HEAD: BEGIN SECTIONS HERE

Case I showing more dispersion than the average for the random D's, for example in Figure 15. The mean flux at 60 cm is more nearly a step function for Case II than for Case I. Examining the 180-cm flux in Figure 17, we see the breakthrough is delayed and a sigmoid curve has developed, but again Case II is less dispersed. Results for the velocity under a pulse input are consistent (Figures 16 and 18).

Results with varying velocities (Cases III-VI) are considerably different. These were also run with a Monte Carlo procedure, but with v selected randomly. Examining the five-day concentration curves for varying v's in Figure 13, one observes immediately that the shapes tend to be hyperbolic rather than sigmoid. The concentrations at deep depths are more than for the constant cases, the salt is spread out more on the average with no sharply defined front. This is a consequence of the greatly skewed distribution of v. The profiles where v is higher, have salt to greater depths than for the mean v; similarly, for profiles where v is lower, there is no salt at all reaching the depth corresponding to the mean v. The averaged profiles, then, have higher concentrations deep in the profile, but a much lower concentration where before we had a front for Cases I and II. The velocity pattern dominates the step-input case, and even when D = 0 (Case III), the same shape is found.

The effect of increasing D = 0 (Case III) to the mean value of 378 cm^2/day (Case IV) can be observed in Figure 13 for the variable v. The latter results are for higher concentrations for any given depth, the consequence of salt moving ahead of the step-input case. When D is variable and independent of the variable v (Case V), the resulting profile is in between, again showing the effect of the variable D, to be similar to a D smaller than the mean value. When D increases with the variable v by Equation 65 (Case VI), the resulting mean is almost directly on top of the zero D curve. Thus, for highly correlated D and v values, the effect of larger D's are ineffective in dispersing the average curves, since the larger D's are small for the shallow fronts.

Results of varying v's on the pulse input calculations are also considerably different than for constant v's. The maximum of the mean curves is much more shallow, with long tails downward due to the fast velocity profiles. The calculated mean fluxes are also different. The front side of the breakthrough curve is difficult to detect and the back side has a long tail, corresponding to the low velocity profiles which are late to dissipate.

The depth of the maximum value of c/c_o as a function of time and depth is calculated using the simplified Equation 62 and is displayed as Cases I' and II' in Figure 19. (Only results for constant v and pulses are given.) The values for the deterministic Case I' are less for all depths (or equivalently, times). The mean values for varying D are considerably greater due to the many "profiles" with D values less than the mean D, hence they disperse more slowly. The shaded area shows the range of $(c/c_o)_{max}$ between the 25th and 75th percentile value of D. The 75th percentile value is to the left (but still above the deterministic results); the 25th percentile value

BEGIN LAST LINE OF TEXT
BOTTOM OF IMAGE AREA. OUTSIDE DIMENSION FOR TABLES AND ILLUSTRATIONS
3/8"

EPA-287 (Cin.)
(4-76)

is to the right corresponding to the largest maximum concentrations at any given time.

An overview of the results suggests two pronounced effects:

(1) If a constant velocity is to be used and the D is highly skewed, a D-value much smaller than the mean D should be used. The mean D will give more dispersion than occurs on the average.

(2) The variable v results in greatly different average profiles than a deterministic calculation. The variable v calculations show the average salt fronts are hyperbolic for the lower reaches of a pulse input. A D value which increases directly with velocity, gives almost the same average as for D = 0 for a step input.

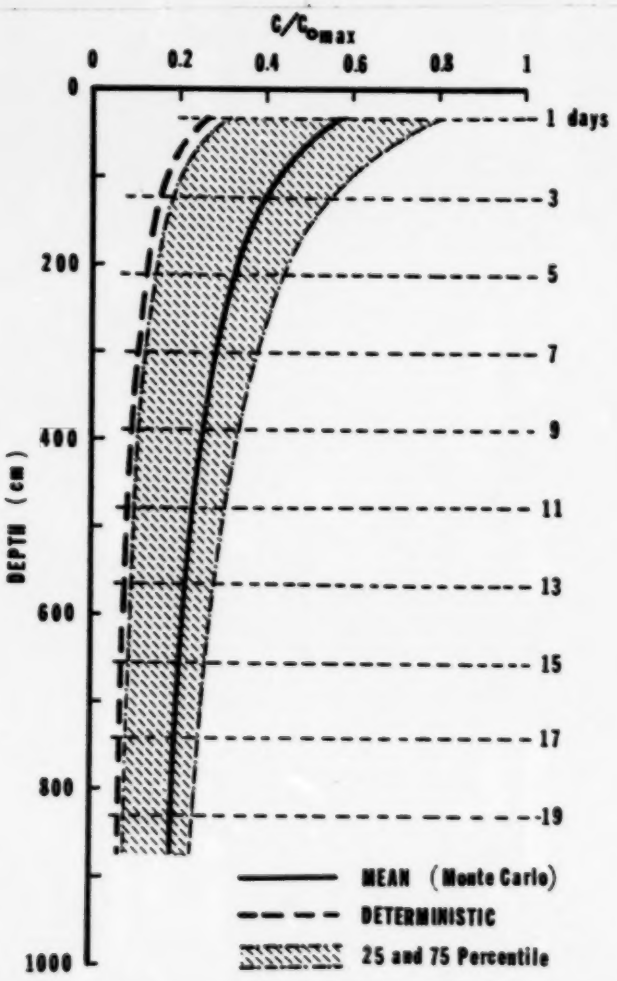

Figure 19. Values of $(c/c_o)_{max}$ for v = 44.3 cm/day and random apparent diffusion coefficient (Example 1).

BEGIN FIRST LINE OF TEXT HERE
TYPING GUIDE SHEET
CENTER OF PAGE
TOP OF IMAGE AREA
DROPPED HEAD; BEGIN SECTIONS HERE

SECTION 10

SENSITIVITY

Sensitivity is defined as the rate of change of one factor as the result of change in another factor (McCuen, 1973). Mathematically, we can state sensitivity of a dependent variable $f(x_1, x_2, \ldots, x_n)$ with respect to one of its independent variables x_1, $i = 1, 2, \ldots n$ as $\partial f(x_1, x_2, \ldots, x_n)/\partial x_i$. In general, for a differentiable function, the change in f as the result of change in x_i can be obtained using the Taylor series expansion

$$f(x_1, x_2, \ldots, x_i + \Delta x, \ldots, x_n) = f(x_1, x_2, \ldots, x_n) + (\partial f/\partial x_i)\Delta x_i + (\partial^2 f/\partial x_i^2)(\Delta x_i)^2/2 + \ldots \quad (66)$$

If the second and higher order terms are small compared to the linear terms, we have

$$f(x_1, x_2, \ldots x_i + \Delta x_i, \ldots, x_n) = f(x_1, x_2, \ldots, x_n) + (\partial f/\partial x_i)\Delta x_i \quad (67)$$

and the change of f is approximately

$$\Delta f = f(x_1, x_2, \ldots, x_i + \Delta x_i \ldots, x_n) - f(x_1, x_2, \ldots, x) = (\partial f/\partial x_i)\Delta x_i \quad (68)$$

and results in the general equation

$$S_{A,i} = (\partial f/\partial x_i) = \frac{f(x_1, x_2, \ldots, x_i + \Delta x_i, \ldots, x_n) - f(x_i, x_2, \ldots, x_n)}{\Delta x_i} \quad (69)$$

where $S_{A,i}$ is the sensitivity.

When there is a functional relationship (analytical or empirical) between the dependent and independent variables, the analytical derivative is used. For numerical (tabular) relationships, however, the finite difference form of Equation 69 is used.

The value obtained by Equation 69 is usually referred to as absolute sensitivity and is dependent on the magnitude of f and x_i. The absolute sensitivity, therefore, is often not appropriate for the comparison of values. A sensitivity value invariant with respect to the magnitude of the independent and dependent variables can be obtained by considering the relative changes in f with respect to relative changes in x_i (McCuen, 1973, 1974; Colman and DeCoursey, 1976). Thus, the relative sensitivity, $S_{R,i}$ is defined as

BEGIN LAST LINE OF TEXT
BOTTOM OF IMAGE AREA; OUTSIDE DIMENSION FOR TABLES AND ILLUSTRATIONS
3/8"

EPA-287 (Cin.) (4-76)

$$S_{R,i} = (\partial f/\partial x_i)(x_i/f) \quad (70)$$

or

$$S_{R,i} \simeq (\Delta f/\Delta x_i)(x_i/f) \quad (71)$$

The relative sensitivity values are less dependent on the magnitude of x_i and f, and therefore provide a better means for comparing values independent of units and independent of size of the parameters.

Coleman and DeCoursey (1976) introduce another relative sensitivity

$$S^*_{R,i} = (\frac{\Delta f}{\Delta x_i})[\frac{(x_i - x_{io})}{f}] \quad (72)$$

where x_{io} is the minimum value that x_i can assume. They claim that this form is more meaningful when some of the variables which are compared have a range in variability quite different from their numerical value. For example, the range of barometric pressure changes is much less than its magnitude, whereas the temperature range might be higher or smaller than its magnitude.

The sensitivity of the soil water flux to the variation of the soil hydraulic properties were studied relative to individual parameters.

SIMPLE DRAINAGE EQUATION--SENSITIVITY

The simplified drainage equation (Eq. 28) $J_L = K_o/(1 + \alpha^* t K_o/L)$, is considered first. The absolute sensitivity of J_L to K_o and α^* can be found from the following two equations

$$S_{A,K_o} = \partial J_L/\partial K_o = 1/(1 + \alpha^* K_o t/L)^2 \quad (73)$$

and

$$S_{A,\alpha^*} = \partial J_L/\partial \alpha^* = -(K_o{}^2 t/L)/(1 + \alpha^* t K_o/L)^2 \quad (74)$$

The relative sensitivity of J_L to K_o and α^* can be found by appropriate substitutions into Eq. 70. The values of the flux, the absolute and relative sensititives for K_o and α^* for the 180-cm depth are given in Table 9.

At time t = 0, the flux is only a function of K_o and independent of α^*. As t gets larger the value of J_L decreases. The absolute sensitivity for K_o decreases sharply as t gets larger, however the relative sensitivity for K_o decreases less rapidly. For large values of time the relative and absolute sensitivity values for K_o approach zero. The absolute sensitivity of J_L with respect to α^* decreases to a minimum of -0.13 as time gets larger and then moves back toward zero. The relative sensitivity to α^*, on the other hand, shows a continuous decrease towards -1 as t gets large. These indicate that for small values of time, the flux is very sensitive to K_o and less sensitive to α^*. For larger values of time, however, the effects of K_o on the

TABLE 9. THE FLUX J_L, AND THE ABSOLUTE AND RELATIVE SENSITIVITY OF J_L WITH RESPECT TO K_o AND α AS A FUNCTION OF TIME (FOR THE SIMPLIFIED DRAINAGE FORMULA)

t	J_L	S_{A,K_o}	S_{R,K_o}	S_{A,α^*}	S_{R,α^*}
0.0	31.9	1.0	1.0	0.0	0.0
0.05	20.7	0.421	0.649	-0.119	-0.351
0.1	15.3	0.230	0.480	-0.130	-0.520
0.25	8.61	0.073	0.270	-0.103	-0.730
0.50	4.97	0.024	0.156	-0.069	-0.844
1	2.70	0.007	0.085	-0.040	-0.915
2	1.41	0.002	0.044	-0.022	-0.956
5	0.58	0.000	0.018	-0.009	-0.982
10	0.29	0.000	0.009	-0.005	-0.991
20	0.15	0.000	0.005	-0.002	-0.995
∞*	0.0	0.0	0.0	0.0	-1.0

* The simplified drainage equation, Eq. 28, is not valid as $t \to \infty$. We show these values for illustration only.

J_L value decreases, whereas the effects of α^* become more important.

NON-LINEAR DRAINAGE--SENSITIVITY

The sensitivity of the non-linear flow equation to the various soil parameters may also be evaluated. The partial derivative of Eq. 61 may be approximated by the finite difference form. Two examples are considered: (a) the Panoche loam using the moisture characteristic data and hydraulic conductivity function of Warrick (1975) and (b) the Yolo after Haverkamp et al. (1977). The original data in both cases was collected at the University of California, Davis.

The boundary condition after time t = 0 is that no flow occurs across the surface. The initial condition is a constant water content.

Example 1. The soil water characteristic for the Panoche is from Warrick (1975, Table 1)

$$h = -1300 \exp(-10.5\,\theta), \qquad \theta < 0.36$$

$$= -(1.59)(10)^7 \exp(-36.6\,\theta), \qquad \theta > 0.36 \tag{75}$$

BEGIN FIRST LINE OF TEXT HERE
TYPING GUIDE SHEET
CENTER OF PAGE
TOP OF IMAGE AREA
DROPPED HEAD; BEGIN SECTIONS HERE

The unsaturated hydraulic conductivity is taken as

$$K = K_o \exp(\alpha^* h),$$

$$K_o = 95 \text{ cm/day}$$

$$\alpha^* = 0.04 \text{ cm}^{-1} \qquad (76)$$

The sensitivity of the soil water flux and moisture content is evaluated with respect to K_o and the slope factor α^*. Table 10 contains results of the sensitivities of specific flux for various times and at 4 and 60 cm. Note the flux values at 4 cm are much smaller (because the top of the profile has been more depleted of water. We note that the absolute sensitivities (S_{A,K_o} and S_{A,α^*}) differ greatly with time, with depth and with the parameter studied. Magnitudes range from approximately 10^{-5} to 800. This is, to a large extent, a reflection of magnitudes and units. The effect is nullified by using the relative sensitivities (S_{R,K_o} and S_{R,α^*}) which reduce the range to about 0.0 to 1.0. The most sensitive results correspond to the fastest flux values. There is an interesting sign change (positive to negative) for small times with respect to K_o. This results because the fluxes are initially larger for large K_o, but the profile drains faster when the surface flux drops to zero for higher K_o.

Table 11 shows results for moisture content θ. The initial θ was 0.45. The moisture content is much more sensitive to α^* for larger times, whereas for small times they are approximately the same.

Example 2. The soil water characteristic for Yolo as used by Haverkamp et al. (1977) is

$$K = K_o[A/(A + |h|^{\beta})] \qquad \text{(cm/hr)}$$

$$K_o = (4.428)(10)^{-2}, \; A = 124.6, \; \beta = 1.77 \qquad (77)$$

The unsaturated hydraulic conductivity is

$$\theta = \theta_r + a(\theta_s - \theta_r)/[a + (\ln|h|)^{\beta}]$$

$$\theta_s = 0.495, \; \theta_r = 0.124, \quad a = 739, \quad \beta = 4 \text{ for } h < -1 \text{ cm}$$

$$\theta = \theta_s, \quad h \geq -1 \text{ cm} \qquad (78)$$

Sensitivity of the specific flux, J_L, to K_o are shown in Table 12 for 4 and 60 cm. At both depths the values decrease with time. The shallower depth (4 cm) damps towards zero faster because the upper profile drains first. The moisture contents are less sensitive to K_o as shown by Table 13. Note the negative values, again larger K_o would lead to a faster depletion.

BEGIN LAST LINE OF TEXT
BOTTOM OF IMAGE AREA; OUTSIDE DIMENSION FOR TABLES AND ILLUSTRATIONS
3/8"

EPA-287 (Cin.)
(4-76).

TABLE 10. SENSITIVITY OF THE SPECIFIC FLUX, J_L, TO K_o AND α^* FOR PANOCHE. VALUES ARE CALCULATED AT K_o = 0.95 cm/day AND α^* = 0.04 cm^{-1} (see Equations 75 and 76)

t (hours)	4 cm					60 cm				
	Flux J_L(cm/da)	S_{A,K_o}	S_{R,K_o}	S_{A,α^*}	S_{R,α^*}	Flux J_L(cm/da)	S_{A,K_o}	S_{R,K_o}	S_{A,α^*}	S_{R,α^*}
.5	5.42	.0128	.224	-55.8	-.412	28.7	.291	.962	-821	-1.14
6	.673	.000379	.0535	- 6.61	-.393	8.50	.000628	.00701	- 94.2	- .446
12	.337	-.000203	-.0572	- 3.61	-.429	4.03	-.00645	-.152	- 39.1	- .388
18	.216	-.000268	-.118	- 2.35	-.435	2.49	-.00564	-.215	- 22.3	- .359
24	.155	-.000250	-.153	- 1.64	-.424	1.74	-.00449	-.244	- 14.5	- .332
30	.119	-.000217	-.173	- 1.21	-.407	1.31	-.00357	-.258	- 10.1	- .308
36	.0960	-.000188	-.186	- .951	-.396	1.04	-.00289	-.263	- 7.52	- .288
42	.0799	-.000163	-.194	- .770	-.385	.858	-.00240	-.265	- 5.83	- .272
48	.0682	-.000143	-.199	- .639	-.375	.725	-.00202	-.265	- 4.68	- .258
60	.0522	-.000112	-.203	- .466	-.357	.546	-.00150	-.261	- 3.23	- .236
90	.0321	-.0000682	-.202	- .261	-.326	.329	-.000859	-.248	- 1.66	- .201
120	.0227	-.0000471	-.197	- .174	-.306	.230	-.000573	-.237	- 1.04	- .180
148	.0177	-.0000358	-.192	- .129	-.292	.178	-.000426	-.228	- .740	- .167

TABLE 11. SENSITIVITY OF VOLUMETRIC MOISTURE CONTENT, θ, TO K_o AND α^* FOR PANOCHE. VALUES ARE CALCULATED AT K_o = 95 cm/day AND α^* = 0.04 cm^{-1} (see Equations 75 and 76)

t (hours)	4 cm					60 cm				
	θ (cm^3/cm^3)	S_{A,K_o}	S_{R,K_o}	S_{A,α^*}	S_{R,α^*}	θ (cm^3/cm^3)	S_{A,K_o}	S_{R,K_o}	S_{A,α^*}	S_{R,α^*}
.5	.327	-.000190	-.0551	0.60	.0734	.360	0	0	.025	.00278
6	.266	-.000295	-.105	1.30	.196	.310	-.000432	-.133	1.38	.118
12	.246	-.000295	-.114	1.53	.248	.281	-.000421	-.143	1.7	.242
18	.235	-.000274	-.111	1.63	.276	.265	-.000379	-.136	1.85	.279
24	.228	-.000263	-.110	1.70	.299	.255	-.000358	-.133	1.93	.302
30	.222	-.000242	-.103	1.78	.319	.248	-.000326	-.125	2.00	.323
36	.218	-.000232	-.101	1.80	.330	.242	-.000316	-.124	2.03	.335
42	.215	-.000232	-.103	1.83	.340	.237	-.000295	-.118	2.05	.345
48	.212	-.000232	-.104	1.85	.350	.234	-.000284	-.116	2.08	.355
60	.207	-.000211	-.0965	1.90	.367	.228	-.000274	-.114	2.10	.366
90	.199	-.000190	-.0903	1.95	.391	.218	0.000242	-.106	2.15	.395
120	.194	-.000190	-.0927	1.98	.407	.212	-.000221	-.0992	2.18	.411
148	.191	-.000179	-.0892	2.00	.419	.207	-.000211	-.0964	2.20	.425

BEGIN FIRST LINE OF TEXT HERE
TYPING GUIDE SHEET
CENTER OF PAGE
TOP OF IMAGE AREA
DROPPED HEAD: BEGIN SECTIONS HERE

TABLE 12. SENSITIVITY OF THE SPECIFIC FLUX, J_L, TO K_o FOR YOLO SOIL, VALUES ARE CALCULATED AT K_o = 0.0443 cm/hr (see Equations 77 and 78)

t (hours)	4 cm			60 cm		
	Flux J_L(cm/da)	S_{A,K_o}	S_{R,K_o}	Flux J_L(cm/da)	S_{A,K_o}	S_{R,K_o}
0.5	.307	.269	.931	.330	.310	1.00
6	.175	.0892	.541	.330	.310	1.00
12	.122	.0483	.421	.329	.310	.999
18	.0955	.0333	.371	.329	.307	.992
24	.0793	.0255	.341	.328	.301	.975
30	.0683	.0205	.320	.325	.290	.948
36	.0603	.0172	.303	.321	.276	.913
42	.0541	.0148	.290	.316	.260	.874
48	.0492	.0129	.278	.310	.243	.832
60	.0418	.0102	.260	.296	.201	.752
90	.0308	.00651	.225	.260	.144	.593
120	.0246	.00462	.200	.228	.104	.486
148	.0208	.00353	.181	.203	.0795	.417

BEGIN LAST LINE OF TEXT
3/8"
BOTTOM OF IMAGE AREA, OUTSIDE DIMENSION FOR TABLES AND ILLUSTRATIONS

EPA-287 (Cin.) (4-76)

TABLE 13. SENSITIVITY OF THE VOLUMETRIC WATER CONTENT, θ, TO K_o FOR THE YOLO SOIL. VALUES ARE CALCULATED AT K_o = 0.0443 cm/hr (see Equations 77 and 78)

t (hours)	4 cm			60 cm		
	$\theta(cm^3/cm^3)$	S_{A,K_o}	S_{R,K_o}	$\theta(cm^3/cm^3)$	S_{A,K_o}	S_{R,K_o}
0.5	.449	-.000941	-.00223	.450	0	0
6	.442	-.00565	-.0136	.450	0	0
12	.437	-.00847	-.0206	.450	0	0
18	.433	-.00941	-.0231	.450	0	0
24	.430	-.0113	-.0279	.450	-.000941	-.0222
30	.428	-.0122	-.0304	.450	-.000941	-.00222
36	.425	-.0132	-.0329	.450	-.000941	-.00222
42	.423	-.0141	-.0355	.449	-.00188	-.00445
48	.421	-.0141	-.0356	.449	-.00282	-.00668
60	.418	-.0151	-.0383	.448	-.00471	-.0112
90	.411	-.0179	-.0463	.445	-.00941	-.0225
120	.405	-.0188	-.0494	.441	-.0132	-.0317
148	.401	-.0198	-.0524	.438	-.0169	-.0411

REFERENCES

Biggar, J.W. and D.R. Nielsen. 1976. Spatial variability of the leaching characteristics of a field soil. Water Resources Res. 12:78-84.

Blyth, J.F. and D.A. Macleod. 1978. The significance of soil variability in northeast Scotland. J. Soil Sci. 29:419-430.

Cameron, D.R. 1978. Variability of soil water retention curves and predicted hydraulic conductivities on a small plot. Soil Sci. 126:364-371.

Carvallo, H.O., D.K. Cassel, J. Hammond, and A. Bauer. 1976. Spatial variability of *in situ* unsaturated hydraulic conductivity of Maddock sandy loam. Soil Sci. 121:1-7.

Cassel, D.K. and A. Bauer. 1975. Spatial variability in soils below depth of tillage. Bulk density and fifteen atmosphere percentage. Soil Sci. Soc. Amer. Proc. 39:247-250.

Coelho, M.A. Spatial variability of water related soil physical parameters. 1974. Ph.D. Dissertation. Univ. of Ariz., Tucson. 110 pp. (Available as 75-11,061 from Xerox University Microfilms, Ann Arbor, Mich. 48106).

Coleman, G. and D.G. DeCoursey. 1976. Sensitivity and model variance analysis applied to some evaporation and evapotranspiration models. Water Resources Res. 12:873-879.

Elrick, D.E., J.H. Scandrett, and E.E. Miller. 1959. Tests of capillary flow scaling. Soil Sci. Soc. Amer. Proc. 23:329-332.

Gumaa, G.S. 1978. Spatial variability of *in situ* available water. Ph.D. Dissertation, the Univ. of Ariz. 140 pp. (Available as 78-24,365 from Xerox University microfilms, Ann Arbor, Mich. 48106.)

Hammersly, J.M. and D.C. Handscomb. 1964. Monte Carlo Methods. Metheun and Co., London.

Haverkamp, R., M. Vauclin, J. Touma, P.J. Wierenga, and G. Vachaud. 1977. A comparison of numerical simulation models for one-dimensional infiltration. Soil Sci. Soc. Amer. J. 41:285-294.

Journel, A.G. and C.J. Huijbregts. 1978. Mining geostatistics. Academic Press, New York. 600 pp.

Keisling, T.C. 1974. Precision with which selected physical properties of similar soils can be measured. Ph.D. Dissertation. Okla. State Univ. 108 pp. (Available as 75-8812 from Xerox University microfilms, Ann Arbor, Mich. 48106.)

Kirkham, D., and W.L. Powers. 1972. Advanced soil physics. John Wiley, New York. 534 pp.

Kleijnen, J.P.C. 1974. Statistical techniques in simulation: Part 1. Marcel-Dekker, Inc., New York. 775 pp.

Klute, A., and G.E. Wilkinson. 1958. Some tests of the similar media concept of capillary flow. I. Reduced capillary conductivity and moisture characteristic data. Soil Sci. Soc. Amer. Proc. 22:278-281.

Maisel, H. and G. Gnugnoli. 1972. Simulation of discrete stochastic systems. Sci. Res. Assoc., Inc., Chicago. 465 pp.

McCuen, R.H. 1973. The role of sensitivity analysis in hydrologic modeling. J. Hydrology 18:37-53.

McCuen, R.H. 1974. A sensitivity and error analysis of procedures used for estimating evaporation and evapotranspiration models. Water Resources Res. 12:873-879.

Miller, E.E., and R.D. Miller. 1955. Theory of capillary flow. I. Practical implications. Soil Sci. Soc. Amer. Proc. 19:267-271.

Miller, E.E., and R.D. Miller. 1956. Physical theory for capillary flow phenomena. J. Appl. Phys. 27:324-332.

Miller, R.D., and E.E. Miller. 1955. Theory of capillary flow. II. Experimental information. Soil Sci. Soc. Amer. Proc. 19:271-275.

Nielsen, D.R., J.W. Biggar, and K.T. Erh. 1973. Spatial variability of field measured soil-water properties. Hilgardia 42:215-259.

Petersen, R.G. and L.D. Calvin. 1965. Sampling. In C.A. Black (ed.) Methods of Soil Analysis, Part 1. Amer. Soc. Agron. Madison, Wis. 777 pp.

Philip, J.R. 1957. The theory of infiltration. I. The infiltration equation and its solution. Soil Sci. 83:345-357.

Philip, J.R. 1967. Sorption and infiltration in heterogeneous media. Aust. J. Soil Res. 5:1-10.

Philip, J.R. 1969. Theory of infiltration. Advan. Hydrosci. 5:215-305.

Rao, P.S.C., P.V. Rao and J.M. Davidson. 1977. Estimation of the spatial variability of the soil water flux. Soil Sci. Soc. of Amer. J. 41:1208-1209.

Rubin, J., and R. Steinhardt. 1963. Soil water relations during rain infiltration. I. Theory. Soil Sci. Soc. Amer. Proc. 26:246-251.

Simmons, C.S., D.R. Nielsen, and J.W. Biggar. 1980. Scaling of field measured water properties. Hilgardia 47:77-174.

Van de Pol, R.M., P.J. Wierenga, and D.R. Nielsen. 1977. Solute movement in a field soil. Soil Sci. Soc. Amer. J. 41:10-13.

Wagenet, R.J. and J.J. Jurinak. 1978. Spatial variability of soluble salt content in a Mancos shale watershed. Soil Sci. 126:342-349.

Warrick, A.W. 1975. Analytical solutions to the one-dimensional linearized moisture flow equation for arbitrary input. Soil Sci. 120:79-84.

Warrick, A.W. 1977. Areal predictions of soil water flux in the unsaturated zone. Proc. Irrig. Return Flow Conf., May 16-19, Fort Collins, p 225-231.

Warrick, A.W., J.W. Biggar and D.R. Nielsen. 1971. Simultaneous solute and water transfer for an unsaturated soil. Water Resour. Res. 7:1216-1225.

Warrick, A.W., G.J. Mullen, and D.R. Nielsen. 1977a. Scaling field-measured soil hydraulic properties using a similar media concept. Water Resour. Res. 13:355-362.

Warrick, A.W., G.J. Mullen, and D.R. Nielsen. 1977b. Predictions of the soil water flux based upon field-measured soil-water properties. Soil Sci. Soc. Amer. J. 41:14-19.

Webster, R. 1977. Spectral analysis of gilgai soil. Aust. J. Soil Res. 15: 191-204.

Williamson, L.S. and R.L. Hurst. 1965. Sample size estimates in permeability studies. J. Irrig. and Drain Div. Amer. Soc. Civil Eng. 91:1-9.

Wilkinson, G.E., and A.Klute. 1959. Some tests of the similar media concept of capillary flow, II. Flow systems data. Soil Sci. Soc. Amer. Proc. 23: 434-437.

PUBLICATIONS AND PAPERS ASSOCIATED WITH RESULTS

Published Papers

Warrick, A.W. 1977. Areal predictions of soil water flux in the unsaturated zone. Proc. Irrig. Return Flow Conference, May 16-19, Fort Collins, p. 225-231.

Warrick, A.W. and A. Amoozegar-Fard. 1979. Infiltration and drainage calculations using spatially scaled hydraulic properties. Water Resources Res. 15:1116-1120.

Paper Presentations

Amoozegar-Fard, A. and A.W. Warrick. 1979. Dissipation of soil solutes for spatially-variable apparent diffusion coefficients. Annual Meeting of Soil Sci. Soc. Amer., Fort Collins, Aug. 5-10, Fort Collins, Colorado.

Warrick, A.W. and A. Amoozegar-Fard. 1979. Scaling areal soil moisture distributions for drainage and high frequency surface irrigation. Annual Meeting of Soil Sci. Soc. Amer., Aug. 5-10, Fort Collins, Colorado.

Papers in Preparation

Amoozegar-Fard, A., A.W. Warrick, and D.R. Nielsen. 1980. Solute movement in spatially-varying flow velocities and apparent diffusion coefficients. (To be submitted to Soil Sci. Soc. Amer. J.)

Warrick, A.W. and A. Amoozegar-Fard. 1980. Scaling soil water patterns for high frequency irrigation. (To be submitted to Soil Sci.)

BEGIN FIRST LINE OF TEXT HERE
TYPING GUIDE SHEET
CENTER OF PAGE
TOP OF IMAGE AREA
DROPPED HEAD BEGIN SECTIONS HERE

APPENDIX

FINITE DIFFERENCE PROGRAM--FLUX SPECIFIED AT BOUNDARY

```
     PROGRAM MOISTRS    74/74   OPT=0 TRACE                    FTN 4.6+428

  1                  PROGRAM MOISTRS(INPUT,OUTPUT)
                     COMMON/BLK1/ A(51), B(51),C(51),D(51), THETA(51)
                     COMMON/BLK2/ TETSA
                     DIMENSION X(100)
  5                  REAL   KOLD, KNEW, MIN

                C
                C    ****************************************************************
                C    *                                                              *
 10             C    *  FINITE DIFFERENCE PROGRAM FOR INFILTRATION, DRAINAGE OR     *
                C    *  CYCLIC WATER APPLICATION.                                   *
                C    *                          BY                                  *
                C    *            A. AMOOZEGAR-FARD, AND A. W. WARRICK              *
                C    *         DEPARTMENT OF SOILS, WATER AND ENGINEERING            *
 15             C    *                  UNIVERSITY OF ARIZONA                       *
                C    *                                                              *
                C    ****************************************************************
                C
                C    THE PROGRAM SOLVES THE NON-LINEAR MOISTURE FLOW EQUATION FOR
 20             C    INFILTRATION, DRAINAGE OR CYCLIC WATER APPLICATIONS.  CRANK-
                C    NICOLSON SCHEME IS USED ( REMSON, I., G. M. HORNBERGER, AND
                C    F. J. MOLZ.  1971.  NUMERICAL METHODS IN SUBSURFACE HYDROLOGY
                C    WITH AN INTRODUCTION TO THE FINITE ELEMENT METHOD.  JOHN WIELY
                C    AND SONS INC.  NEW YORK. ) AND THE GRIDS ARE PLACED IN SUCH
 25             C    A WAY THAT THE LINE X = 0 COINCIDES WITH THE 1/2 GRID POINT
                C    ( RUBIN, J. AND R. STEINHARDT.  1963.  SOIL WATER RELATIONS
                C    DURING RAIN INFILTRATION: I. THEORY.  SOIL SCI. SOC. AMER.
                C    PROC. 26,246-251. ).  THE SPACE INCREMENT, DELTA X, IS CONSTANT
                C    WHEREAS THE TIME INCREMENT, DELTA T, CAN BE INCREASED WITH
 30             C    TIME.
                C    THOMAS ALGORITHM ( VON ROSENBERG, D. U.. 1969.  METHODS FOR THE
                C    NUMERICAL SOLUTION OF PARTIAL DIFFERENTIAL EQUATIONS.  AMERICAN
                C    ELSEVIER PUBLISHING CO. INC.  NEW YORK. ) IS USED TO SOLVE
                C    THE DIAGONAL MATRIX.  THE HYDRAULIC CONDUCTIVITY AND THE
 35             C    SPECIFIC WATER CAPACITY ( D THETA/ D H) ARE GIVEN AS "FUNCTION"
                C    SUBROUTINES.
                C    THE UPPER BOUNDRY CONDITION IS GIVEN AS FLUX ACROSS THE SOIL
                C    SURFACE AND THE LOWER BOUNDRY CONDITION IS UNIT HYDRAULIC
                C    GRADIENT.
 40             C      1. INTEGRATING THE MOISTURE PROFILE
                C      2. CALCULATING THE STORAGE BY INFLOW - OUTFLOW
                C    MASS BALANCE IS DONE BY :
                C    THE UNITS ARE CM FOR SPACE AND DAYS FOR TIME.
```

BEGIN LAST LINE OF TEXT
BOTTOM OF IMAGE AREA OUTSIDE DIMENSION FOR TABLES AND ILLUSTRATIONS
3/8"

PAGE NUMBER
EPA-287 (Cm)
(4-76)

BEGIN FIRST LINE OF TEXT HERE
TYPING GUIDE SHEET
CENTER OF PAGE
TOP OF IMAGE AREA
DROPPED HEAD, BEGIN SECTIONS HERE

```
      PROGRAM MOISIRS    74/74   OPT=0 TRACE                    FTN 4.6+428


                C
 45             C       ******************
                C       THE VARIABLES ARE
                C       ******************
                C
                C       TM                      CONSTANT TO CONVERT MINUTES TO DAY, 1440
 50             C       TCYCLE                  LENGTH OF THE CYCLE IN CYCLIC CASE, UNITS
                C                               MINUTES
                C       TWET, TDRY              LENGTH OF WATER APPLICATION AND DRAINAGE
                C                               PERIODS RESPECTIVELY, UNITS MINUTES
                C       NCYCLE                  CYCLE NUMBER
 55             C       T0, T1,T2,...., TN      POINTS IN THE TIME TO CHANGE THE DELTA T
                C       N                       NUMBER OF SPACE INCREMENTS
                C       DX                      DELTA X, UNITS CM
                C       TDEL                    DELTA T, UNITS MINUTES
                C       DELT                    DELTA T, UNITS DAYS
 60             C       WETV                    FLUX ACROSS THE SURFACE IN INFILTRATION OR
                C                               DURING WATER APPLICATION IN CYCLIC CASE
                C       DRYV                    FLUX ACROSS THE SURFACE IN DRAINAGE OR
                C                               DURING THE DRAINAGE PERIOD OF THE CYCLIC CASE
                C       TETAS                   SATURATED WATER CONTENT
 65             C       TETIN                   INITIAL WATER CONTENT
                C       T                       TIME, UNITS MINUTES
                C       X                       VERTICAL DISTANSE, UNITS CM
                C       STOR                    THE AMOUNT OF WATER STORED IN THE PROFILE
                C                               CALCULATED BY : STORAGE = INFLOW - OUTFLOW
 70             C       CALST                   THE AMOUNT OF WATER STORED IN THE PROFILE
                C                               CALCULATED BY INTEGRATING THE MOISTURE
                C                               PROFILE
                C       INK, KNT, AND IA        CONSTANTS USED FOR PRINTING THE
                C                               RESULTS EVERY SO OFTEN
 75             C

                      TM = 1440.
                      TCYCLE = 12.*60.
                      TWET = 12.*60.
 80                   TDRY = TCYCLE-TWET
                      T0=0.5
                      T1=179.99
                      T2=359.99
                      T3=659.99
 85                   T4=899.99
                      T5=1199.99
                      N=20
                      TDEL=0.5
                      DX=4.
 90                   WETV=0.001306*86400.
                      DRYV=0.0
                      TETSA=0.397
                      TETIN=0.005

 95                   DO       2      I=1,N
                2     THETA(I)=TETIN
                      THETA(N+1)=TETIN

                      X(1)=0.0
```

BEGIN LAST LINE OF TEXT
BOTTOM OF IMAGE AREA, OUTSIDE DIMENSION FOR TABLES AND ILLUSTRATIONS
3/8"

EPA-287 (Cin.)
(4-76)

BEGIN FIRST LINE OF TEXT HERE

CENTER OF PAGE

TOP OF IMAGE AREA

DROPPED HEAD; BEGIN SECTIONS HERE

```
      PROGRAM MOISTRS    74/74   OPT=0 TRACE                    FTN 4.6+428
100                 DO     20     I=1,N
                    LI=I+2
                    X(LI)=(I-0.5)*DX
                    X(LI+1)= I*DX
                20  CONTINUE
105
                    T=0.0
                    STOR = 0.0
                    VOLD=COND(THETA(N))
                    TNK=0.
110                 KNT=0.
                    WRITE      25
                25  FORMAT(1H1)

              C
115           C     ***** START OF THE CALCULATIONS *****
              C

                    DO     100     L=1,500
                    TA=1.
120                 FLUX=DRYV
                    NCYCLE = T/TCYCLE
                    TT= T-TCYCLE*NCYCLE
                    TA=1.
                    IF(TT.LT.TWET)     FLUX=WETV
125                 IF(TT-TWET)     30,35,40
                30  NT=0.0
                    GO TO 41
                35  TDEL=0.5
                    TA=10.
130                 GO TO 49
                40  NT=1
                41  TN=TT-NT*TWET
                    TDEL=0.5
                    TNK=(T+TDEL)/20.
135                 IF(TN.LT.T1)     GO TO 42
                    TDEL=1.
                    TNK=(T+TDEL)/20.
                    IF(TN.LT.T2)          GO TO 42
                    TDEL=2.
140                 TNK=(T+TDEL)/20.
                    IF(TN.LT.T3)          GO TO 42
                    TDEL=3.
                    TNK=(T+TDEL)/20.
                    IF(TN.LT.T4)          GO TO 42
145                 TDEL=5.
                    TNK=(T+TDEL)/20.
                    IF(TN.LT.T5)          GO TO 42
                    TDEL=10.
                    TNK=(T+TDEL)/20.
150             42  IF(ABS(TWET-TT).LT.TDEL)       TDEL=ABS(TWET-TT)
                    IF(ABS(TCYCLE-TT).LT.TDEL)     TDEL=ABS(TCYCLE-TT)
                    KNT=TNK+0.00001
                    IF(ABS(TNK-KNT).LT.0.000001)    TA=10.
                49  CONTINUE
155
                    T=T+TDEL
```

BOTTOM OF IMAGE AREA; OUTSIDE DIMENSION FOR TABLES AND ILLUSTRATIONS

BEGIN LAST LINE OF TEXT

3/8"

BEGIN FIRST LINE OF TEXT HERE
TYPING GUIDE SHEET
CENTER OF PAGE
TOP OF IMAGE AREA
DROPPED HEAD; BEGIN SECTIONS HERE

```
      PROGRAM MOISTRS    74/74   OPT=0 TRACE                    FTN 4.6+428

                      DELT=TDEL/TM

                      DTDX=DELT/(2.*DX*DX)
  160                 TNEW=(THETA(1)+THETA(2))/ 2.
                      KNEW=COND(TNEW)
                      CNEW=CF(TNEW)

                      A(1)=0.
  165                 C(1)= DTDX*KNEW/CNEW
                      B(1)= -1.-C(1)
                      D(1)= -THETA(1)-C(1)*(THETA(2)-THETA(1)) + DELT/DX*(KNEW-FLUX)

                      THETA(N+1)= THETA(N)
  170
                      DO     50      I=2,N
                      TOLD=TNEW
                      KOLD=KNEW
                      COLD=CNEW
  175                 TNEW= (THETA(I)+THETA(I+1))/2.
                      KNEW= COND(TNEW)
                      CNEW=CF(TNEW)
                      IN2=2*I

  180                 A(I)=DTDX*KOLD/COLD
                      C(I)= DTDX*KNEW/CNEW
                      B(I) = -1.-A(I)-C(I)
                      D(I) = -THETA(I) -C(I)*(THETA(I+1)-THETA(I))+A(I)*
                     *  (THETA(I)-THETA(I-1)) + DELT/DX*(KNEW-KOLD)
  185
                50    CONTINUE
                      B(N)= B(N)+C(N)

                      CALL THOM(N)

  190
                      N2=2*N
                      VNEW=COND(THETA(N))
                      VFLUX=(VOLD+VNEW)/2.
                      VNET=FLUX-VFLUX
  195                 STOR= STOR+VNET*DELT
                      VOLD=VNEW

                      IF(TA.LT.5.)          GO TO 90
                      NHOUR=T/60. +0.000001
  200                 MIN=T-NHOUR*60.
                59    WRITE     60,      NHOUR, MIN
                60    FORMAT(///, 20X*FOR TIME*5X,I6* HOUR(S) AND*F10.2
                     *  MINUTE(S)*//)
                      WRITE      65
  205           65    FORMAT(30X*X* 13X*THETA*13X*FLUX*/)
                      CALST = 0.0
                      DO      80     I=1,N
                      IN=2*I
                      FLUX2 = 0.0
  210                 RK = COND(THETA(I))
                      RC = CF(THETA(I))
                      IF(I.EQ.1)        GO TO 68
                      FLUX2 = RK/RC*(THETA(I+1)-THETA(I-1))/(2.*DX) - RK
```

BOTTOM OF IMAGE AREA; OUTSIDE DIMENSION FOR TABLES AND ILLUSTRATIONS
BEGIN LAST LINE OF TEXT
3/8"

EPA-287 (Cin.)
(4-76)

BEGIN FIRST LINE OF TEXT HERE

TYPING GUIDE SHEET

CENTER OF PAGE

TOP OF IMAGE AREA

DROPPED HEAD; BEGIN SECTIONS HERE

```
      PROGRAM MOISTRS    74/74   OPT=0 TRACE                    FTN 4.6+428

                     GO TO 69
215                68  FLUX2=RK/RC*(THETA(I+1)-THETA(I))/DX-RK
                   69  WRITE     70,   X(IN), THETA(I), FLUX2
                   70  FORMAT(25X,2(F10.5,5X),F15.8)
                       CALST = CALST + (THETA(I)-TETIN) * DX
                   80  CONTINUE
220                    DIFF = CALST - STOR
                       WRITE  86,     CALST, STOR   , DIFF
                   86  FORMAT(/,20X*THE STORAGE CALCULATED BY INTEGRATION IS    *F10.5,
                      *  /20X*THE STORAGE CALCULATED BY INFLOW - OUTFLOW IS*F10.5,/,20X
                      *  *THE DIFFERENCE IS                                *F10.5,//)
225                90  CONTINUE
                  100  CONTINUE
                       STOP
                       END
```

BEGIN LAST LINE OF TEXT

BOTTOM OF IMAGE AREA; OUTSIDE DIMENSION FOR TABLES AND ILLUSTRATIONS

3/8"

EPA-287 (Cin.)
(4-76)

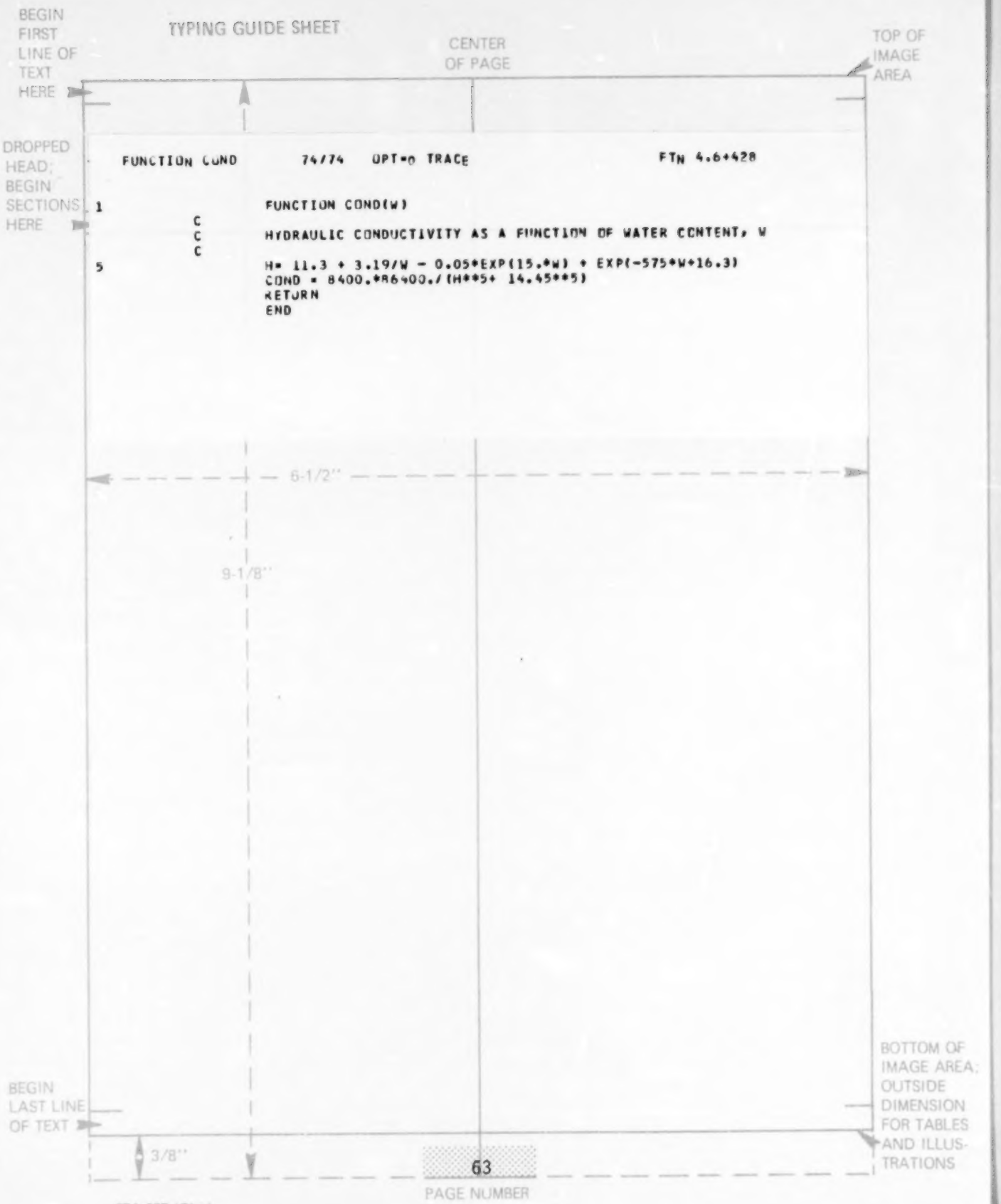
BEGIN FIRST LINE OF TEXT HERE
TYPING GUIDE SHEET
CENTER OF PAGE
TOP OF IMAGE AREA
DROPPED HEAD; BEGIN SECTIONS HERE
FUNCTION COND 74/74 OPT=0 TRACE FTN 4.6+428
1 FUNCTION COND(W)
C
C HYDRAULIC CONDUCTIVITY AS A FUNCTION OF WATER CONTENT, W
C
5 H= 11.3 + 3.19/W - 0.05*EXP(15.*W) + EXP(-575*W+16.3)
COND = 8400.*86400./(H**5+ 14.45**5)
RETURN
END
6-1/2"
9-1/8"
BEGIN LAST LINE OF TEXT
BOTTOM OF IMAGE AREA; OUTSIDE DIMENSION FOR TABLES AND ILLUSTRATIONS
3/8"
63
PAGE NUMBER
EPA-287 (Cin.)
(4-76)

BEGIN FIRST LINE OF TEXT HERE
TYPING GUIDE SHEET
CENTER OF PAGE
TOP OF IMAGE AREA
DROPPED HEAD; BEGIN SECTIONS HERE
FUNCTION CF 74/74 OPT=0 TRACE FTN 4.6+442
1 FUNCTION CF(W)
C
C SPECIFIC WATER CAPACITY AS A FUNCTION OF WATER CONTENT, W
C
5 DHDTE = -3.19/(W*W) - 0.75*EXP(15.*W) - 575*EXP(-575*W+16.3)
CF= -1./DHDTE
RETURN
END
6-1/2"
9-1/8"
BEGIN LAST LINE OF TEXT
BOTTOM OF IMAGE AREA; OUTSIDE DIMENSION FOR TABLES AND ILLUSTRATIONS
3/8"
64
PAGE NUMBER
EPA-287 (Cin.)
(4-76)

TYPING GUIDE SHEET

BEGIN FIRST LINE OF TEXT HERE

CENTER OF PAGE

TOP OF IMAGE AREA

DROPPED HEAD; BEGIN SECTIONS HERE

```
 SUBROUTINE THOM       74/74   OPT=0 TRACE                    FTN 4.6+428

 1                    SUBROUTINE  THOM(N)
                C
                C     THOMAS ALGORITHM
                C
 5                    COMMON/BLK1/ A(51), B(51),C(51),D(51), THETA(51)
                     DIMENSION   BETA(51),GAMA (51)
                     A(1)=0.0
                     C(N)=0.0
                     BETA(1)=B(1)
10                   GAMA(1)=D(1)/B(1)
                     DO     10 I=2,N
                     BETA(I)= B(I)-A(I)*C(I-1)/BETA(I-1)
                     GAMA(I)=(   D(I)-A(I)*GAMA(I-1))/BETA(I)
               10    CONTINUE
15                   THETA(N)=GAMA(N)
                     M=N-1
                     DO     20     J=1,M
                     I=N-J
                     THETA(I)= GAMA(I)-C(I)*THETA(I+1)/ BETA(I)
20             20    CONTINUE
                     RETURN
                     END
```

BEGIN LAST LINE OF TEXT

BOTTOM OF IMAGE AREA; OUTSIDE DIMENSION FOR TABLES AND ILLUSTRATIONS

3/8"

EPA-287 (Cin.)
(4-76)

TYPING GUIDE SHEET
FIRST LINE OF TEXT HERE
CENTER OF PAGE
TOP OF IMAGE AREA
DROPPED HEAD: BEGIN SECTIONS HERE

FOR TIME 0 HOUR(S) AND 20.00 MINUTE(S)

X	THETA	FLUX
2.00000	.21200	-144.36813456
6.00000	.16146	-105.43149428
10.00000	.03333	-2.99465928
14.00000	.00500	-.00000000
18.00000	.00500	-.00000000
22.00000	.00500	-.00000000
26.00000	.00500	-.00000000
30.00000	.00500	-.00000000
34.00000	.00500	-.00000000
38.00000	.00500	-.00000000
42.00000	.00500	-.00000000
46.00000	.00500	-.00000000
50.00000	.00500	-.00000000
54.00000	.00500	-.00000000
58.00000	.00500	-.00000000
62.00000	.00500	-.00000000
66.00000	.00500	-.00000000
70.00000	.00500	-.00000000
74.00000	.00500	-.00000000
78.00000	.00500	-.00000000

THE STORAGE CALCULATED BY INTEGRATION IS 1.56720
THE STORAGE CALCULATED BY INFLOW - OUTFLOW IS 1.56720
THE DIFFERENCE IS -.00000

FOR TIME 0 HOUR(S) AND 40.00 MINUTE(S)

X	THETA	FLUX
2.00000	.23434	-120.56151716
6.00000	.22336	-113.57842384
10.00000	.19817	-110.91866196
14.00000	.13460	-73.31308981
18.00000	.01813	-.05346154
22.00000	.00500	-.00000000
26.00000	.00500	-.00000000
30.00000	.00500	-.00000000
34.00000	.00500	-.00000000
38.00000	.00500	-.00000000
42.00000	.00500	-.00000000
46.00000	.00500	-.00000000
50.00000	.00500	-.00000000
54.00000	.00500	-.00000000
58.00000	.00500	-.00000000
62.00000	.00500	-.00000000
66.00000	.00500	-.00000000
70.00000	.00500	-.00000000
74.00000	.00500	-.00000000
78.00000	.00500	-.00000000

THE STORAGE CALCULATED BY INTEGRATION IS 3.13440
THE STORAGE CALCULATED BY INFLOW - OUTFLOW IS 3.13440
THE DIFFERENCE IS -.00000

BEGIN LAST LINE OF TEXT
BOTTOM OF IMAGE AREA; OUTSIDE DIMENSION FOR TABLES AND ILLUSTRATIONS
3/8"

EPA-287 (Cin.)
(4-76)

BEGIN FIRST LINE OF TEXT HERE
TYPING GUIDE SHEET
CENTER OF PAGE
TOP OF IMAGE AREA
DROPPED HEAD: BEGIN SECTIONS HERE

FOR TIME 1 HOUR(S) AND 0.00 MINUTE(S)

X	THETA	FLUX
2.00000	.24008	-115.13324239
6.00000	.23680	-112.76734991
10.00000	.23007	-111.59490284
14.00000	.21584	-108.71868565
18.00000	.18427	-108.85300670
22.00000	.09541	-36.33485532
26.00000	.00794	-.00000000
30.00000	.00500	-.00000000
34.00000	.00500	-.00000000
38.00000	.00500	-.00000000
42.00000	.00500	-.00000000
46.00000	.00500	-.00000000
50.00000	.00500	-.00000000
54.00000	.00500	-.00000000
58.00000	.00500	-.00000000
62.00000	.00500	-.00000000
66.00000	.00500	-.00000000
70.00000	.00500	-.00000000
74.00000	.00500	-.00000000
78.00000	.00500	-.00000000

THE STORAGE CALCULATED BY INTEGRATION IS 4.70160
THE STORAGE CALCULATED BY INFLOW - OUTFLOW IS 4.70160
THE DIFFERENCE IS -.00000

FOR TIME 1 HOUR(S) AND 20.00 MINUTE(S)

X	THETA	FLUX
2.00000	.24190	-113.59600546
6.00000	.24082	-112.79647793
10.00000	.23857	-112.39701827
14.00000	.23437	-111.57174836
18.00000	.22556	-109.77841819
22.00000	.20683	-104.26848043
26.00000	.16652	-101.41065867
30.00000	.05226	-9.07020916
34.00000	.00526	-.00000000
38.00000	.00500	-.00000000
42.00000	.00500	-.00000000
46.00000	.00500	-.00000000
50.00000	.00500	-.00000000
54.00000	.00500	-.00000000
58.00000	.00500	-.00000000
62.00000	.00500	-.00000000
66.00000	.00500	-.00000000
70.00000	.00500	-.00000000
74.00000	.00500	-.00000000
78.00000	.00500	-.00000000

THE STORAGE CALCULATED BY INTEGRATION IS 6.26880
THE STORAGE CALCULATED BY INFLOW - OUTFLOW IS 6.26880
THE DIFFERENCE IS -.00000

BEGIN LAST LINE OF TEXT
BOTTOM OF IMAGE AREA; OUTSIDE DIMENSION FOR TABLES AND ILLUSTRATIONS
3/8"

EPA-287 (Cin.)
(4-76)

BEGIN FIRST LINE OF TEXT HERE
TYPING GUIDE SHEET
CENTER OF PAGE
TOP OF IMAGE AREA
DROPPED HEAD; BEGIN SECTIONS HERE

FOR TIME 1 HOUR(S) AND 40.00 MINUTE(S)

X	THETA	FLUX
2.00000	.24251	-113.09562413
6.00000	.24214	-112.81948929
10.00000	.24142	-112.67256414
14.00000	.24002	-112.36666228
18.00000	.23725	-111.76749622
22.00000	.23172	-110.64773333
26.00000	.22030	-108.47598095
30.00000	.19535	-103.04424083
34.00000	.13726	-74.28169648
38.00000	.02103	-.85269105
42.00000	.00500	-.00000000
46.00000	.00500	-.00000000
50.00000	.00500	-.00000000
54.00000	.00500	-.00000000
58.00000	.00500	-.00000000
62.00000	.00500	-.00000000
66.00000	.00500	-.00000000
70.00000	.00500	-.00000000
74.00000	.00500	-.00000000
78.00000	.00500	-.00000000

THE STORAGE CALCULATED BY INTEGRATION IS 7.83600
THE STORAGE CALCULATED BY INFLOW - OUTFLOW IS 7.83600
THE DIFFERENCE IS -.00000

FOR TIME 2 HOUR(S) AND 0.00 MINUTE(S)

X	THETA	FLUX
2.00000	.24272	-112.92692088
6.00000	.24259	-112.83166795
10.00000	.24235	-112.78063772
14.00000	.24187	-112.67333725
18.00000	.24094	-112.45755000
22.00000	.23913	-112.03459317
26.00000	.23559	-111.21612009
30.00000	.22850	-109.60651027
34.00000	.21381	-106.04557658
38.00000	.18489	-105.31403692
42.00000	.09360	-34.54752238
46.00000	.00781	-.00000000
50.00000	.00500	-.00000000
54.00000	.00500	-.00000000
58.00000	.00500	-.00000000
62.00000	.00500	-.00000000
66.00000	.00500	-.00000000
70.00000	.00500	-.00000000
74.00000	.00500	-.00000000
78.00000	.00500	-.00000000

THE STORAGE CALCULATED BY INTEGRATION IS 9.40320
THE STORAGE CALCULATED BY INFLOW - OUTFLOW IS 9.40320
THE DIFFERENCE IS -.00000

BEGIN LAST LINE OF TEXT
BOTTOM OF IMAGE AREA OUTSIDE DIMENSION FOR TABLES AND ILLUSTRATIONS
3/8"

EPA-287 (Cin.)
(4-76)

BEGIN FIRST LINE OF TEXT HERE
TYPING GUIDE SHEET
CENTER OF PAGE
TOP OF IMAGE AREA
DROPPED HEAD; BEGIN SECTIONS HERE

FOR TIME 2 HOUR(S) AND 20.00 MINUTE(S)

X	THETA	FLUX
2.00000	.24279	-112.86899170
6.00000	.24275	-112.83602763
10.00000	.24266	-112.81824660
14.00000	.24250	-112.78069911
18.00000	.24218	-112.70492212
22.00000	.24157	-112.55041166
26.00000	.24039	-112.27191895
30.00000	.23809	-111.73722432
34.00000	.23356	-110.73624250
38.00000	.22436	-108.69095813
42.00000	.20492	-102.67276261
46.00000	.16344	-98.31199248
50.00000	.04822	-7.38298827
54.00000	.00518	-.00000000
58.00000	.00500	-.00000000
62.00000	.00500	-.00000000
66.00000	.00500	-.00000000
70.00000	.00500	-.00000000
74.00000	.00500	-.00000000
78.00000	.00500	-.00000000

THE STORAGE CALCULATED BY INTEGRATION IS 10.97040
THE STORAGE CALCULATED BY INFLOW - OUTFLOW IS 10.97040
THE DIFFERENCE IS -.00000

FOR TIME 2 HOUR(S) AND 40.00 MINUTE(S)

X	THETA	FLUX
2.00000	.24282	-112.84899194
6.00000	.24280	-112.83757931
10.00000	.24277	-112.83142418
14.00000	.24271	-112.81841329
18.00000	.24261	-112.79206950
22.00000	.24239	-112.74003494
26.00000	.24199	-112.63883509
30.00000	.24122	-112.44432814
34.00000	.23972	-112.07531775
38.00000	.23682	-111.38861632
42.00000	.23105	-110.13924499
46.00000	.21916	-107.76447775
50.00000	.19323	-102.60686537
54.00000	.13186	-68.78545864
58.00000	.01825	-.06190918
62.00000	.00500	-.00000000
66.00000	.00500	-.00000000
70.00000	.00500	-.00000000
74.00000	.00500	-.00000000
78.00000	.00500	-.00000000

THE STORAGE CALCULATED BY INTEGRATION IS 12.53760
THE STORAGE CALCULATED BY INFLOW - OUTFLOW IS 12.53760
THE DIFFERENCE IS -.00000

BEGIN LAST LINE OF TEXT
BOTTOM OF IMAGE AREA, OUTSIDE DIMENSION FOR TABLES AND ILLUSTRATIONS
3/8"

EPA-287 (Cin.)
(4-76)

BEGIN FIRST LINE OF TEXT HERE
TYPING GUIDE SHEET
CENTER OF PAGE
TOP OF IMAGE AREA
DROPPED HEAD; BEGIN SECTIONS HERE

FOR TIME 3 HOUR(S) AND 0.00 MINUTE(S)

X	THETA	FLUX
2.00000	.24283	-112.84207031
6.00000	.24282	-112.83811604
10.00000	.24281	-112.83598267
14.00000	.24279	-112.83146931
18.00000	.24275	-112.82232296
22.00000	.24268	-112.80424519
26.00000	.24254	-112.76907454
30.00000	.24227	-112.70139014
34.00000	.24176	-112.57217870
38.00000	.24079	-112.32698626
42.00000	.23889	-111.86334814
46.00000	.23520	-110.98359812
50.00000	.22780	-109.25081989
54.00000	.21248	-105.76928615
58.00000	.17942	-104.98916447
62.00000	.08636	-29.03174972
66.00000	.00701	-.00000000
70.00000	.00500	-.00000000
74.00000	.00500	-.00000000
78.00000	.00500	-.00000000

THE STORAGE CALCULATED BY INTEGRATION IS 14.10480
THE STORAGE CALCULATED BY INFLOW - OUTFLOW IS 14.10480
THE DIFFERENCE IS -.00000

FOR TIME 3 HOUR(S) AND 20.00 MINUTE(S)

X	THETA	FLUX
2.00000	.24283	-112.83962400
6.00000	.24283	-112.83835934
10.00000	.24282	-112.83768796
14.00000	.24282	-112.83625117
18.00000	.24280	-112.83332486
22.00000	.24278	-112.82753008
26.00000	.24274	-112.81674998
30.00000	.24265	-112.79453633
34.00000	.24248	-112.75308016
38.00000	.24217	-112.67451827
42.00000	.24156	-112.52694693
46.00000	.24039	-112.25320879
50.00000	.23811	-111.75454752
54.00000	.23357	-110.86057864
58.00000	.22426	-109.14112492
62.00000	.20423	-104.04705504
66.00000	.15985	-97.37541731
70.00000	.03911	-4.37260765
74.00000	.00500	-.00000000
78.00000	.00500	-.00000000

THE STORAGE CALCULATED BY INTEGRATION IS 15.67200
THE STORAGE CALCULATED BY INFLOW - OUTFLOW IS 15.67200
THE DIFFERENCE IS -.00000

BEGIN LAST LINE OF TEXT
BOTTOM OF IMAGE AREA, OUTSIDE DIMENSION FOR TABLES AND ILLUSTRATIONS
3/8"

EPA-287 (Cin.)
(4-76)

BEGIN FIRST LINE OF TEXT HERE
TYPING GUIDE SHEET
CENTER OF PAGE
TOP OF IMAGE AREA
DROPPED HEAD; BEGIN SECTIONS HERE

FOR TIME 3 HOUR(S) AND 40.00 MINUTE(S)

X	THETA	FLUX
2.00000	.24283	-112.83879684
6.00000	.24283	-112.83839070
10.00000	.24283	-112.83817931
14.00000	.24283	-112.83772601
18.00000	.24282	-112.83680139
22.00000	.24281	-112.83496835
26.00000	.24280	-112.83139626
30.00000	.24277	-112.82450937
34.00000	.24272	-112.81132129
38.00000	.24261	-112.78617504
42.00000	.24241	-112.73836317
46.00000	.24202	-112.64767838
50.00000	.24127	-112.47635475
54.00000	.23982	-112.15559558
58.00000	.23697	-111.56676456
62.00000	.23123	-110.51770950
66.00000	.21926	-108.58240719
70.00000	.19263	-107.23012807
74.00000	.12291	-61.04352587
78.00000	.01343	-.00000585

THE STORAGE CALCULATED BY INTEGRATION IS 17.23920
THE STORAGE CALCULATED BY INFLOW - OUTFLOW IS 17.23920
THE DIFFERENCE IS -.00000

FOR TIME 4 HOUR(S) AND 0.00 MINUTE(S)

X	THETA	FLUX
2.00000	.24283	-112.83853156
6.00000	.24283	-112.83839834
10.00000	.24283	-112.83833123
14.00000	.24283	-112.83818694
18.00000	.24283	-112.83789139
22.00000	.24282	-112.83730356
26.00000	.24282	-112.83615315
30.00000	.24281	-112.83392363
34.00000	.24279	-112.82962687
38.00000	.24276	-112.82136900
42.00000	.24269	-112.80550730
46.00000	.24256	-112.77498916
50.00000	.24231	-112.71598399
54.00000	.24183	-112.60067776
58.00000	.24090	-112.37037668
62.00000	.23911	-111.88967447
66.00000	.23565	-110.79203349
70.00000	.22898	-107.79916982
74.00000	.21666	-97.39666186
78.00000	.19903	-70.12521981

THE STORAGE CALCULATED BY INTEGRATION IS 18.63140
THE STORAGE CALCULATED BY INFLOW - OUTFLOW IS 18.61246
THE DIFFERENCE IS .01894

BEGIN LAST LINE OF TEXT
BOTTOM OF IMAGE AREA; OUTSIDE DIMENSION FOR TABLES AND ILLUSTRATIONS
3/8"

EPA-287 (Cin.)
(4-76)

BEGIN FIRST LINE OF TEXT HERE
TYPING GUIDE SHEET
CENTER OF PAGE
TOP OF IMAGE AREA
DROPPED HEAD; BEGIN SECTIONS HERE

FOR TIME 4 HOUR(S) AND 20.00 MINUTE(S)

X	THETA	FLUX
2.00000	.24283	-112.83844368
6.00000	.24283	-112.83839956
10.00000	.24283	-112.83837727
14.00000	.24283	-112.83832864
18.00000	.24283	-112.83822712
22.00000	.24283	-112.83801951
26.00000	.24283	-112.83759807
30.00000	.24282	-112.83674208
34.00000	.24282	-112.83499448
38.00000	.24281	-112.83140209
42.00000	.24279	-112.82397393
46.00000	.24275	-112.80857498
50.00000	.24269	-112.77673684
54.00000	.24257	-112.71151924
58.00000	.24237	-112.58015775
62.00000	.24205	-112.32218308
66.00000	.24155	-111.83323128
70.00000	.24087	-110.95148648
74.00000	.24003	-109.47351210
78.00000	.23931	-107.72701695

THE STORAGE CALCULATED BY INTEGRATION IS 18.98086
THE STORAGE CALCULATED BY INFLOW - OUTFLOW IS 18.94389
THE DIFFERENCE IS .03697

FOR TIME 4 HOUR(S) AND 40.00 MINUTE(S)

X	THETA	FLUX
2.00000	.24283	-112.83841366
6.00000	.24283	-112.83839895
10.00000	.24283	-112.83839006
14.00000	.24283	-112.83837045
18.00000	.24283	-112.83832900
22.00000	.24283	-112.83824345
26.00000	.24283	-112.83806975
30.00000	.24283	-112.83772163
34.00000	.24283	-112.83703255
38.00000	.24282	-112.83568746
42.00000	.24282	-112.83310165
46.00000	.24281	-112.82822032
50.00000	.24280	-112.81919790
54.00000	.24278	-112.80292359
58.00000	.24275	-112.77438522
62.00000	.24270	-112.72595126
66.00000	.24263	-112.64684628
70.00000	.24255	-112.52346894
74.00000	.24246	-112.34181652
78.00000	.24238	-112.14679173

THE STORAGE CALCULATED BY INTEGRATION IS 19.01986
THE STORAGE CALCULATED BY INFLOW - OUTFLOW IS 18.98097
THE DIFFERENCE IS .03889

BEGIN LAST LINE OF TEXT
BOTTOM OF IMAGE AREA, OUTSIDE DIMENSION FOR TABLES AND ILLUSTRATIONS
3/8"

EPA-287 (Cin.)
(4-76)

BEGIN FIRST LINE OF TEXT HERE
TYPING GUIDE SHEET
CENTER OF PAGE
TOP OF IMAGE AREA
DROPPED HEAD; BEGIN SECTIONS HERE

FOR TIME 5 HOUR(S) AND 0.00 MINUTE(S)

X	THETA	FLUX
2.00000	.24283	-112.83840373
6.00000	.24283	-112.83839924
10.00000	.24283	-112.83839595
14.00000	.24283	-112.83838893
18.00000	.24283	-112.83837464
22.00000	.24283	-112.83834641
26.00000	.24283	-112.83829186
30.00000	.24283	-112.83818848
34.00000	.24283	-112.83799603
38.00000	.24283	-112.83764408
42.00000	.24283	-112.83701220
46.00000	.24283	-112.83589978
50.00000	.24282	-112.83398248
54.00000	.24282	-112.83075366
58.00000	.24281	-112.82545410
62.00000	.24281	-112.81700337
66.00000	.24280	-112.80396706
70.00000	.24278	-112.78462985
74.00000	.24277	-112.75730174
78.00000	.24276	-112.72072558

THE STORAGE CALCULATED BY INTEGRATION IS 19.02531
THE STORAGE CALCULATED BY INFLOW - OUTFLOW IS 18.98617
THE DIFFERENCE IS .03913

FOR TIME 5 HOUR(S) AND 20.00 MINUTE(S)

X	THETA	FLUX
2.00000	.24283	-112.83840091
6.00000	.24283	-112.83839971
10.00000	.24283	-112.83839873
14.00000	.24283	-112.83839670
18.00000	.24283	-112.83839272
22.00000	.24283	-112.83838513
26.00000	.24283	-112.83837105
30.00000	.24283	-112.83834547
34.00000	.24283	-112.83829986
38.00000	.24283	-112.83821998
42.00000	.24283	-112.83808258
46.00000	.24283	-112.83785059
50.00000	.24283	-112.83746648
54.00000	.24283	-112.83684373
58.00000	.24283	-112.83585706
62.00000	.24283	-112.83433353
66.00000	.24282	-112.83204936
70.00000	.24282	-112.82874244
74.00000	.24282	-112.82415823
78.00000	.24282	-112.81942040

THE STORAGE CALCULATED BY INTEGRATION IS 19.02619
THE STORAGE CALCULATED BY INFLOW - OUTFLOW IS 18.98702
THE DIFFERENCE IS .03917

BEGIN LAST LINE OF TEXT
BOTTOM OF IMAGE AREA; OUTSIDE DIMENSION FOR TABLES AND ILLUSTRATIONS
3/8"

EPA-287 (Cin.)
(4-76)